

Université du Québec
Institut National de la Recherche Scientifique
Centre Armand-Frappier Santé et Biotechnologie

Optimization of techniques for structure-function relationship studies of galectin-13

Par

Carolina PERUSQUÍA HERNÁNDEZ

Mémoire présenté pour l'obtention du grade de
Maître ès sciences (M. Sc.)
en Microbiologie appliquée

Jury d'évaluation

Présidente du jury et
examinatrice interne

Cathy Vaillancourt
Centre Armand-Frappier
Santé et Biotechnologie

Examinatrice externe

Sachiko Sato
Centre de recherche du CHU de
Québec – Université de Laval

Directeur de recherche

Nicolas Doucet
Centre Armand-Frappier
Santé et Biotechnologie

Acknowledgements

I am grateful to Pr. Nicolas Doucet, who accepted me as a student in his research group.

I would like to thank NSERC CREATE-APRENTICE program, not just for funding my graduate studies for two years, but also because being part of the trainees team allow me to commute with nice people from all over Canada, and to discover joy of remote courses even before the pandemic arose. Is still a wonderful experience that enlarged my knowledge and protein science vision.

Thanks to all of those people who were directly involved in development of this project: To Myriam Létourneau, who was always there, and from whom I learnt what does it meant to aid others unconditionally.

To Prof. Cathy Vaillancourt for her patience and assistance to this neophyte in her field of expertise; as well as, to the beautiful people of her group, specially to Josianne, to Linda and to my favorite argentine: Tomás.

To members of Prof. Yves St-Pierre, who also illustrate and guide my first steps working with human cell lines, to Marlène for share with me tricks and accurate advises, to Philippine and, especially to PhD. Camille Fuselier, whose knowledge and expertise have saved me, more than once.

Thanks to PhD. Yossef López de los Santos, who remained me the huge meaning of a tiny monosyllable.

Finally, I am grateful to those with whom I always discussed about lab work and whose discussions also brought light that guided the progress of this project: David, Andrés, Ceci, Noé, Emmanuel, Mustafa.

No mauikalua, no yolmauikalua ua no tlasoj yolikniua, tlasojkamati achi miyek. Ni mits uika no yolko. Mo ueyilnamikilmej nech tlauli sentel maske ti itstokaj uejkapa tlalmej, sentel iuan nee. Ni kin tlasojtlilia. Ometeotl.

Abstract

Prototype galectins are functionally versatile proteins that form homodimers through their carbohydrate recognition domain, CRD, a conserved beta sandwich globular fold that binds β -galactosides. Galectin-13, GAL13, is a unique family member: it dimerizes through two disulfide bridges which link 16-kDa protomers. GAL13 (also called placental protein 13, PP13) is temporarily expressed during pregnancy and is involved in placental invasion and maternal uterine arteries remodeling. Abnormal concentrations of GAL13 in pregnant woman blood serum, are associated with diseases, i.e., pre-eclampsia, miscarriage, and gestational diabetes mellitus. By understanding molecular mechanisms controlling GAL13 biological activities, the design of selective and specific galectin inhibitors could be facilitated. Through this work we established conditions of various techniques forming the basis to study GAL13 structure-function relationship as well as introduced point mutations into the protein glycan binding site, GBS, to prepare GAL13 variants. Hence, we over-expressed and purified non-tagged recombinant GAL13, performed a set of experiments using the glycoprotein asialofetuin, ASF, to evaluate GAL13 binding activity, cell proliferation with JEG-3 cells, from human placental choriocarcinoma, as well as vasodilation assay of rat aortas.

Key words:

Galectin-13, Placental Protein 13, Galectins, purification, characterization, binding

Résumé

Les galectines prototypiques sont des protéines fonctionnellement versatiles qui forment des homodimères grâce à leur domaine de reconnaissance des glucides, CRD, un repliement globulaire conservé qui se lie aux β -galactosides. La galectine-13, GAL13, est un membre unique de la famille : elle se dimérise via deux ponts disulfures qui relient des protomères de 16 kDa. GAL13 (aussi appelé « placental protein 13 », PP13) est temporairement exprimée pendant la grossesse et impliquée dans l'implantation du placenta et le remodelage des artères utérines maternelles. Des concentrations anormales de GAL13 dans le sérum de femme enceinte sont associées à des maladies obstétriques, comme la pré-éclampsie, les fausses couches et le diabète gestationnel mellitus. En comprenant les mécanismes moléculaires contrôlant les activités biologiques de GAL13, la conception d'inhibiteurs de galectine sélectifs et spécifiques pourrait être facilitée. Grâce à ce travail, nous avons établi les conditions des différentes techniques qui constituent la base de l'étude de la relation structure-fonction de GAL13, ainsi que l'introduction de mutations ponctuelles dans le site de liaison des glycans de la protéine, GBS, afin de préparer des variantes mutationnelles de GAL13. Par conséquent, nous avons exprimé et purifié GAL13 recombinante non étiquetée, réalisé une série d'expériences en utilisant la glycoprotéine asialofétuine, ASF, afin d'évaluer l'activité de liaison de GAL13, effectué des essais de prolifération cellulaire avec des cellules de choriocarcinome placentaire humain, JEG-3, en plus d'entreprendre des analyses de vasodilatation des aortes de rat.

Mot clés :

Galectin-13, Placental Protein 13, Galectins, Purification, Caractérisation, Liaison

Table of contents

ACKNOWLEDGEMENTS	II
ABSTRACT	III
RÉSUMÉ	IV
TABLE OF CONTENTS	V
FIGURE INDEX.....	VII
TABLE INDEX.....	IX
ABBREVIATURES	X
INTRODUCTION	1
STRUCTURAL FEATURES OF GALECTINS	2
FUNCTION OF FAMILY MEMBERS.....	6
<i>Galectins: involved in pregnancy</i>	8
GALECTIN-13 AND ITS BIOLOGICAL ROLE	11
RESEARCH PROJECT	16
PROBLEM STATEMENT	16
HYPOTHESIS AND OBJECTIVES.....	19
METHODOLOGY.....	20
1) EXPRESSION AND PURIFICATION OF GAL-13	20
<i>Over-expression</i>	20
<i>Purification</i>	22
2) CHARACTERIZATION OF GAL-13	23
<i>Protein Sequencing</i>	23

<i>SDS-PAGE and Western Blot</i>	24
<i>Mass Spectrometry</i>	25
<i>Circular dichroism (CD)</i>	26
<i>Activity assays</i>	26
3) BINDING ASSAYS WITH GAL-13	29
<i>Fluorescence assay</i>	29
<i>Isothermal Titration Calorimetry (ITC)</i>	29
<i>Microscale Thermophoresis (MST)</i>	30
<i>ELISA</i>	31
RESULTS AND DISCUSSION	32
1) RECOMBINANT GAL-13 PRODUCTION AND PURIFICATION.....	32
1.1) <i>Over-expression</i>	32
1.2) <i>Purification and Quantification</i>	35
2) GAL-13 CHARACTERIZATION	41
2.1) <i>Evaluation of dimerization</i>	41
2.2) <i>Thermal stability of GAL-13</i>	43
2.3) <i>GAL-13 activity</i>	46
3) BINDING ASSAYS	49
4) MUTANTS.....	55
4.1) <i>Over-expression and purification of GBS mutants</i>	57
4.2) <i>Preliminary characterization</i>	59
CONCLUSIONS AND PERSPECTIVES	63
ANNEXES	64
REFERENCES	67

Figure Index

FIGURE 1. CRD OF GALECTIN 13 (5XG7).	2
FIGURE 2. DIMER ARCHITECTURES OF PROTOTYPIC GALECTINS.	4
FIGURE 3. OVERLAY OF CHAIN A FROM HUMAN PROTOTYPE GALECTINS.	5
FIGURE 4. GAL-7 BOUND TO α -LACTOSE (4GAL).	6
FIGURE 5. GALECTINS IN EACH TRIMESTER OF PREGNANCY.	9
FIGURE 6. GALECTIN-13 HOMODIMER (5XG7).	12
FIGURE 7. GAL13 (PP13) MATERNAL SERUM CONCENTRATION DURING PREGNANCY.	13
FIGURE 8. CONSERVED RESIDUES IN CRD OF HUMAN PROTOTYPE GALECTINS.	17
FIGURE 9. PLASMID MAP OF VECTOR PET-22B (+).	32
FIGURE 10. EVALUATION OF GAL-13 OVER-EXPRESSION PROFILES IN DIFFERENT E. COLI STRAINS.	34
FIGURE 11. GAL-13 PURIFICATION ATTEMPT THROUGH ANION EXCHANGE AND SIZE EXCLUSION CHROMATOGRAPHY.	36
FIGURE 12. PURIFICATION OF GAL-13.	38
FIGURE 13. MASS SPECTRUM OF PURIFIED GAL-13.	40
FIGURE 14. REGIONS OF PURIFIED GAL-13 THAT MATCH WITH HUMAN GALECTIN-13 PROTEIN SEQUENCE.	41
FIGURE 15. SEMI-NATIVE SDS-PAGE OF GAL-13.	42
FIGURE 16. CD SPECTRUM OF GAL-13.	43
FIGURE 17. CD MONITORED THERMAL UNFOLDING OF GAL-13.	45
FIGURE 18. RAT AORTA VASODILATION ASSAY.	46
FIGURE 19. INCREASE OF JEG-3 CELLS PROLIFERATION BY GAL-13.	48
FIGURE 20. ISOTHERMAL TITRATION OF GAL-13 WITH LACNAc.	50
FIGURE 21. FLUORESCENCE BINDING ASSAY.	51
FIGURE 22. FLUORESCENCE BINDING ASSAY OF GAL13 WITH ASF.	53
FIGURE 23. DOSE RESPONSE CURVE FROM MST DATA.	54

FIGURE 24. CLOSE UP TO GAL-13'S GBS FROM OVERLAY OF HUMAN PROTOTYPIC GALECTINS. 56

FIGURE 25. PURIFICATION OF GAL-13 MUTANTS. 58

FIGURE 26. CD SPECTRUM OF GAL-13-V63A. 59

FIGURE 27. THERMAL UNFOLDING OF GAL 13-V63A MONITORED BY CD. 60

FIGURE 28. GAL-13-V63A BINDING TOWARDS ASF. 61

FIGURE 29. SEQUENCE ALIGNMENT FROM AN OVERLAY OF GALECTIN STRUCTURES. 64

FIGURE 30. GAL-13 SEC PURIFICATIONS TO ASSESS METHOD REPRODUCIBILITY. 65

FIGURE 31. MS/MS SEQUENCED FRAGMENTS FROM GAL-13 DIGESTION WITH TRYPSIN. 65

FIGURE 32. MST BINDING CHECK OF LACNAC TO GAL-13. 66

FIGURE 34. ITC EXPERIMENT TO CHARACTERIZE GAL-13 BINDING TO ASF. 66

Table Index

TABLE 1. SCHEMATIC REPRESENTATION OF DOMAIN ORGANIZATIONS FOUND IN GALECTINS.	3
TABLE 2. DATA OF PROTOTYPE GALECTINS CRD AMINO ACID SEQUENCE ALIGNMENT FROM STRUCTURAL OVERLAYS. .	4
TABLE 3. DISEASES DURING PREGNANCY WITH ATYPICAL CONCENTRATION OF GAL-13.	14
TABLE 4. PRIMERS USED FOR MUTAGENESIS.	21
TABLE 5. MELTING TEMPERATURE VALUES REPORTED FOR GALECTINS.	45
TABLE 6. DISSOCIATION CONSTANTS REPORTED FOR HUMAN GALECTINS (DAM ET AL., 2005).....	55

Abbreviatures

A	<i>E. coli</i> : Escherichia coli
A, Ala: Alanine	ELISA: Enzyme-linked immunosorbent assay
Ach: Acetylcholine	eNOS: endothelium-derived relaxing factor, member of nitric oxide synthase (NOS) family
Arg: Arginine	
ASF: Asialofetuin	
B	G
BSA: Bovine serum albumin	G, Gly: Glycine
	GalNAc: N-acetyl galactosamine
C	
C, Cys: Cysteine	GAL-1: galectin-1
CD: Circular Dichroism	GAL-2: galectin-2
COM: Center of mass	GAL-3: galectin-3
CRD: Carbohydrate recognition domain	GAL-4: galectin-4
c-Rel: Non glycosylated member of nuclear factor- κ B (NF- κ B) family	GAL-7: galectin-7
	GAL-8: galectin-8
	GAL-9: galectin-9
	GAL-10: galectin-10
	GAL-13: galectin-13
	GAL-14: galectin-14
	GAL-16: galectin-16
D	GBS: glycan binding site
D, Asp: Aspartic acid	H
DNA: desoxiribonucleic acid	H, His: Histidine
E	HELLP: Hemolysis, Elevated Liver enzymes, and Low Platelet count
E, Glu: Glutamic acid	HRP: Horse radish peroxidase

I

I, Ile: Isoleucine

IPTG: isopropyl β -D-thiogalactopyranoside

ITC: Isothermal titration calorimetry

K

K, Lys: Lysine

K_a: Association constant

K_D: Dissociation constant

L

L, Leu: Leucine

LacNAc: N-acetyl lactosamine

LB: Luria-Bertani media

M

M, Met: methionine

m/z: mass charge ratio

mRNA: messenger RNA

MS/MS: tandem mass spectrometry

MST: microscale thermophoresis

N

N, Asn: Asparagine

NK: Natural killer cell

NKT: natural killer T cell

O

O/N: overnight

P

P, Pro: Proline

PAGE: polyacrylamide gel electrophoresis

PDB: Protein data bank

Phe, F: Phenylalanine

PP13: Placental protein 13

PVDF: Polyvinylidene difluoride

Q

Q, Gln: Glutamine

R

R, Arg: Arginine

RNA: Ribonucleic acid

S

S, Ser: Serine

SDS: Sodium dodecyl sulfate

T

T, Thr: threonine

T_m: Melting temperature

Trp, W: Tryptophan

Tyr, Y: Tyrosine

U

UV: Ultraviolet

V

V, Val: valine

ϵ

ϵ : extinction coefficient

λ

λ : wavelength

INTRODUCTION

Galectins are members of the lectin protein family and they have been found widely distributed in eukaryotic taxa (Chan *et al.*, 2018). Nowadays, sixteen members of galectin family have been discovered to be encoded within genomes of mammals, referred to as galectins-1 to -17, twelve sequences of which have been identified in humans (Johannes, Jacob and Leffler, 2018).

Galectins are defined by their affinity towards β -galactoside containing carbohydrates (Vasta *et al.*, 2012), conferring them functional versatility. These proteins are present in numerous locations inside and outside cells (Johannes, Jacob and Leffler, 2018; Laaf *et al.*, 2019). Upon linkage to both glycoproteins and sugar moieties of several molecules, they form a signaling and adhesion network in extracellular matrix (Bartolazzi, 2018).

As glycan binding proteins, galectins are involved in several regulatory processes which allow immune cells to maintain homeostasis. Most family members functions are related to immune cell differentiation and apoptosis through glycan-dependent signaling pathways originating from membrane surface inside cells (Johannes, Jacob and Leffler, 2018).

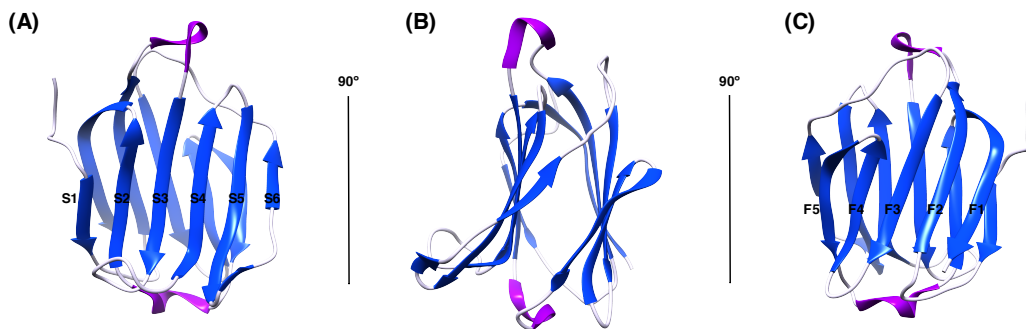
In our research group, we attempt to understand structure-function relationships in galectins to facilitate design of selective and specific inhibitors that promote prognosis and treatment of related diseases.

Structural features of galectins

Galectins are small molecular weight proteins ranging from 14 to 39 kDa. They share a highly conserved three-dimensional fold, known as carbohydrate recognition domain (CRD), with a highly conserved binding pocket or glycan binding site (GBS), responsible for their affinity for β -galactosides (Rabinovich *et al.*, 2002).

CRD of galectins consists of a ~130 amino acid chain that folds as a β -sandwich with an overall jelly-roll topology composed of six (S1 to S6) and five (F1 to F5) β -strands. S-strands form a concave surface where residues implied in ligand binding are located (Figure 1).

Figure 1. CRD of Galectin 13 (5XG7).

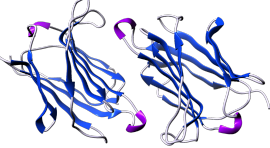
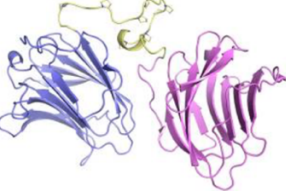
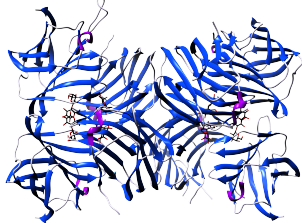


β -strands shown in blue and α -helices in purple, projections show S-strands known as Glycan Binding Site (GBS) in panel (A), a lateral view of jelly-roll in panel (B), and F-strands in panel (C).

Galectins associate and form multimeric species, especially when located in the extracellular matrix (Johannes, Jacob and Leffler, 2018). According to the acquired

architecture when they multimerize, galectins are classified as prototype, tandem repeat and chimeric galectins (Wdowiak *et al.*, 2018) (Table 1).

Table 1. Schematic representation of domain organizations found in galectins.

Subtype	Structure Model	Galectins	Properties
Prototype	 <p>Galectin-10 (1LCL)</p>	-1, -2, -5, -7, -10, -11, -13, -14, -15, -16	Two subunits with the same CRD are linked together non-covalently.
Tandem repeat	 <p>Galectin-4 model taken from (Rustiguel <i>et al.</i>, 2016)</p>	-4, -6, -8, -9, -12	Two CRDs are linked by a functional peptide.
Chimera	 <p>Galectin-3 multimer (6FOF)</p>	3	N-terminal domain with high content in Gly—Pro—Tyr linked to one GBS. Capable of forming multimeric structures.

In tandem-repeat galectins, two distinct CRDs are covalently fused by a functional peptide linker of variable length. Galectin-3 (GAL-3), which is the only chimera type galectin, has just one CRD at C-terminus and a short G-P-Y rich motif at N-terminus, allowing it to form multimeric arrangements like trimers or pentamers. In prototype galectins, dimerization occurs mostly through non-covalent linkage of protomers (Chan *et al.*, 2018; Flores-Ibarra *et al.*, 2018).

Dimerization allows prototype galectins to acquire several three-dimensional arrangements. Figure 2 shows schematic representation and structure of prototype galectins.

Figure 2. Dimer architectures of prototypic galectins.

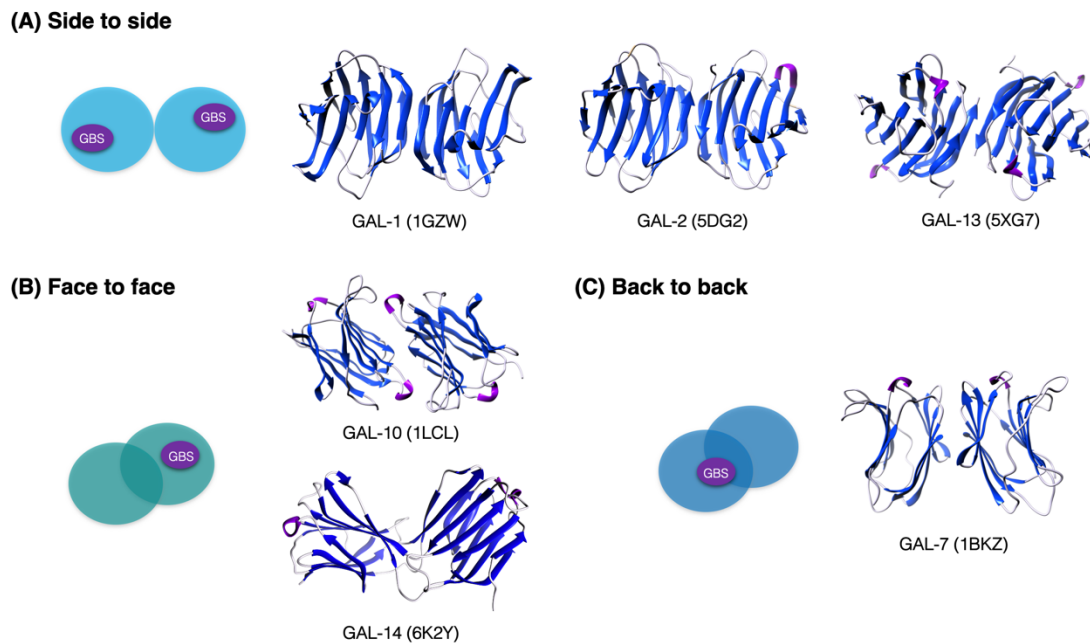


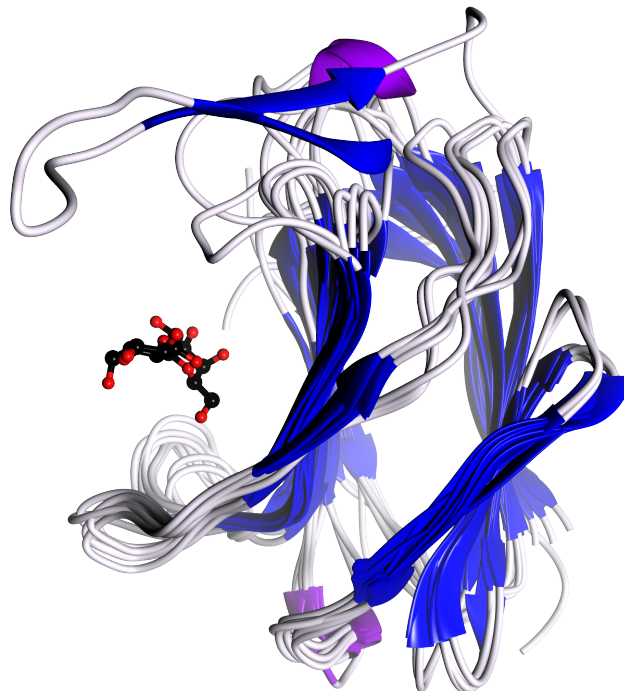
Table 2. Data of prototype galectins CRD amino acid sequence alignment from structural overlays.

Galectin	PDB	Identity to GAL-13 (%)	Coverage (%)
-13	5XG7	NA	NA
-14	6K2Y	67.63	57.1
-16	6LJP	69.78	80.1
-10	1LCL	53.96	92.3
-7	4GAL	28.15	74.9
-2	5DG1	15.62	65.6
-1	1GZW	16.42	55.7

Figure 3 and Table 2 illustrate structural conservation of CRD among galectins, through overlay of one protomer of human galectin-13 (GAL-13) with other human

prototype galectins, made by using UCSF Chimera tools (Pettersen *et al.*, 2004). Superimposed structures have the same characteristic three-dimensional fold and they mainly differ from each other in amino acid composition and the number of residues in their loop regions. In galectins -10 and -13, the loop connecting strands S3 and F2 is extended with four extra residues. CRD of galectin-14 (GAL-14) exhibits major differences: two β -strands (S5 and S6) are extended and are interspersed from one protomer to another to form a dimer (Si, Li, *et al.*, 2021).

Figure 3. Overlay of chain A from human prototype galectins.



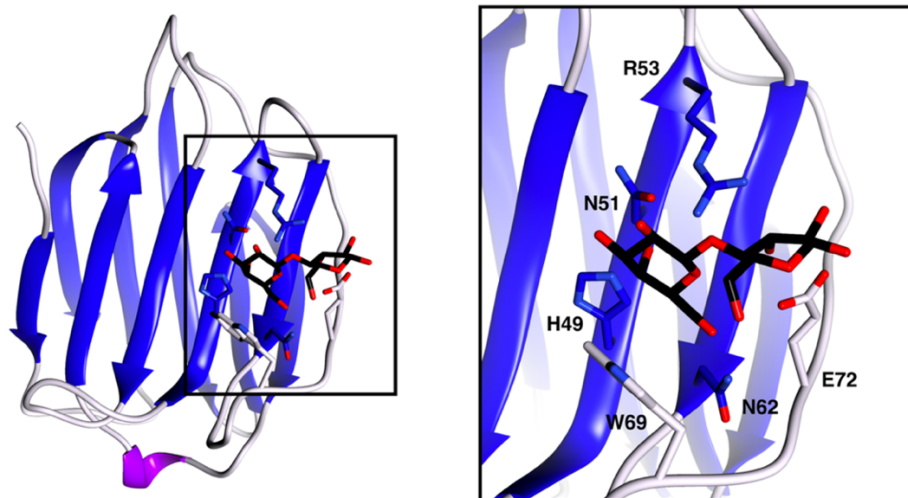
Superimposition of galectins -1 (1GZW), -2 (5DG1), -7 (4GAL), -10 (1LCL), -13 (5XG7), -14 (6K2Y) and -16 (6LJP) was performed with UCSF Chimera (Pettersen *et al.*, 2004), ligand positioning is exemplified by showing β -D-lactose bound to GAL-7 (4GAL) in the GBS.

GBS can recognize different carbohydrates as substrates. Binding interactions can vary according to the ligand because amino acid side chains in galectins' GBS

have been found to rotate and thus, they promote recognition of complex glycans (Leonidas *et al.*, 1998; Saraboji *et al.*, 2012; Miller *et al.*, 2020).

Galectin binding can be exemplified by a closer examination of GAL-7 (Figure 4), because another common feature within the family is positioning of ligand. Residues H49^{hGAL-7}, N51^{hGAL-7}, R53^{hGAL-7}, N62^{hGAL-7} and E72^{hGAL-7} are directly involved in carbohydrate recognition, forming hydrogen bonds with oxygens 4, 5 and 6, respectively, of galactose moiety of ligand. W69^{hGAL07} is involved in stacking interactions with pyranoside ring of galactose.

Figure 4. GAL-7 bound to α -lactose (4GAL).



GBS is located in S4 and S5 strands, residues directly involved in ligand binding are zoomed on right panel.

Function of family members

Galectins are the only glycan binding protein family that can be present in extracellular matrix, cytoplasm, membrane and nucleus, depending on the cell type and cell differentiation state. Therefore, they are involved in a plethora of cellular functions from inter- to intra-cellular signaling pathways that allow cellular growth,

differentiation, and tissue development, as well as gene expression regulation and immune system modulation (Arthur *et al.*, 2015).

Galectins exhibit a diversity of biological activities, either through glycoside binding or GBS independent. Several galectins have functions independent of β -galactoside binding activity (Johannes, Jacob and Leffler, 2018; St-Pierre, Doucet and Chatenet, 2018), which are related to intracellular events. One example is the interaction between B-cell lymphoma 2 (BCL-2) protein with galectins-3 and -7 to promote or inhibit cell apoptosis (Nakahara, Oka and Raz, 2005; Villeneuve *et al.*, 2011).

Through glycan-dependent signaling pathways, galectins are involved in several regulatory processes which allow immune cells to maintain homeostasis, such as immune cell differentiation and apoptosis, T-cell regulation, proliferation and activation, galectins also participate in B-cell differentiation, development, maturation, mobilization and survival. Furthermore, they can also activate natural killer (NK) and natural killer T (NKT) cells, regulate Antigen Presenting Cells, and induce macrophage chemotaxis, activation and differentiation. These proteins have an important role in regulation of granulocytes and mast cells populations, and they are involved in regulation of processes like hemostasis, tissue repair and angiogenesis (Arthur *et al.*, 2015).

Dysregulation of galectin pathways impacts in cellular signaling and it affects neoplastic progression (Arthur *et al.*, 2015). In fact, high galectin expression levels are also associated to mis-regulated cellular functions observed in several human pathologies (Chetry *et al.*, 2018), for example vascular and neoplastic diseases, such as gastric, colorectal, lung, prostate, bladder, breast, head-neck cancers and

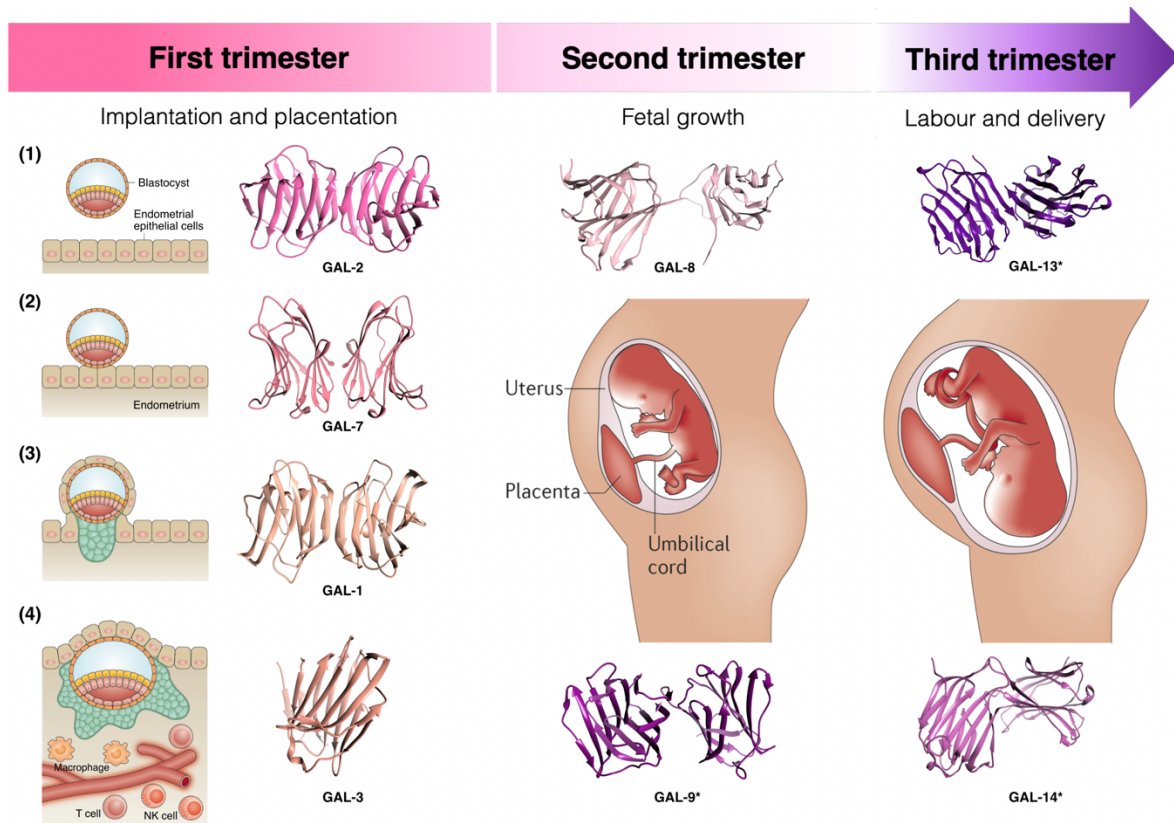
melanoma which have been linked to higher levels of galectin expression (Wdowiak *et al.*, 2018). Moreover, altered functions can vary according to galectin location. Galectin over-expression mainly located inside the cell can cause abnormal cell growth, increase invasive behavior and modulate sensitivity to chemotherapeutic agents. When galectins are outside cells, apoptosis of T-cells can occur, allowing tumor progression or a telogen state in neoplasm-associated macrophages (St-Pierre, Doucet and Chatenet, 2018).

Galectins: involved in pregnancy

From fertilization to the successful birth of a baby, there is a coordination of simultaneous metabolic, endocrine and immune processes. Through glycan binding, members of galectin family, participate in three events which are relevant for pregnancy: signaling to allow cell growth and differentiation, vascular development and immune regulation (Mor, Aldo and Alvero, 2017; Blois *et al.*, 2019).

Medawar's theory strongly influences the role of immunology in pregnancy, in which blastocyst implantation leads to an immunosuppressed state (Trowsdale and Betz, 2006). However, increasing evidence supports the concept that during gestation, evolving immune environment is dynamically modulated (Mor, Aldo and Alvero, 2017). This vision allows us to explain the observed functions of galectin family members during the gestation process (Figure 5) which were reviewed in (Blois *et al.*, 2019).

Figure 5. Galectins in each trimester of pregnancy.



Several galectins were described to participate in specific processes of pregnancy and those marked with an asterisk (*): GAL-9 (2ZHN^{NTD} and 3NV1^{CTD}), GAL-13 (5XG7) and GAL-14 (6K2Y), are thought to be important for all gestation stages. Steps of implantation during first trimester are remarked: (1) Apposition (GAL-2, 5DG1), (2) attachment (GAL-7, 4GAL), (3) invasion (GAL-1, 1GZW), and (4) inflammation (GAL-3, 6FOF). In second trimester, anti-inflammatory response allow fetal development (GAL-8, 2YV8^{NTD} and 2YRO^{CTD}). At the end of third trimester, labor is triggered though inflammatory response (GAL-14, 6K2Y). Modified and adapted from (Mor, Aldo and Alvero, 2017).

Within the first trimester of pregnancy, a pro-inflammatory environment allows implantation of blastocyst. Fertilized blastocyst moves down until it finds surface of epithelial lining of the uterus, this process is known as apposition. GAL-2 activity may be relevant to create a pro-inflammatory environment via polarization of

monocytes and macrophages(Loser *et al.*, 2009); it could also be involved in apposition by interacting with mucins present at the luminal surface of the uterus epithelium, which promotes blastocyst's endometrial receptivity (Blois *et al.*, 2019).

Then, GAL-7 may facilitate adhesion between blastocyst and endometrial epithelium during attachment. Next step, invasion, consists of trophoblast cells penetrating surface of epithelium and invading uterine stroma(Menkhorst *et al.*, 2014). GAL-1 has been proposed to regulate migration of primary trophoblast because it is expressed within most invasive trophoblast cells as it is capable to interact with $\beta 1$ integrin of extra villous trophoblast's membrane (Blois *et al.*, 2019).

Once blastocyst is implanted there is an inflammation step, in which placentation begins by cytotrophoblast proliferation and differentiation to become syncytiotrophoblast; here GAL-1 may affect syncytium formation, as it has been demonstrated to *in vitro* enhance cell migration and invasiveness of both BeWo and mouse trophoblast cells (Fischer *et al.*, 2010; You *et al.*, 2018). GAL03 could be essential for proper implantation, as it participates in activation/differentiation of immune cells in luminal endometrial epithelium, where it is expressed in high concentration (Blois *et al.*, 2019).

In second trimester, an anti-inflammatory milieu promotes fetal growth. GAL-8 might act as an angiogenesis and immune modulator allowing embryo development. At the end of the third trimester, a switch-back to pro-inflammatory is indispensable for labor and delivery (Blois *et al.*, 2019). By interacting with c-Rel, GAL-14 and GAL-16 might play a role in nuclear translocation of nuclear factor- κ B (NF- κ B), whose signaling pathway triggers labor (Si, Li, *et al.*, 2021; Si, Yao, *et al.*, 2021).

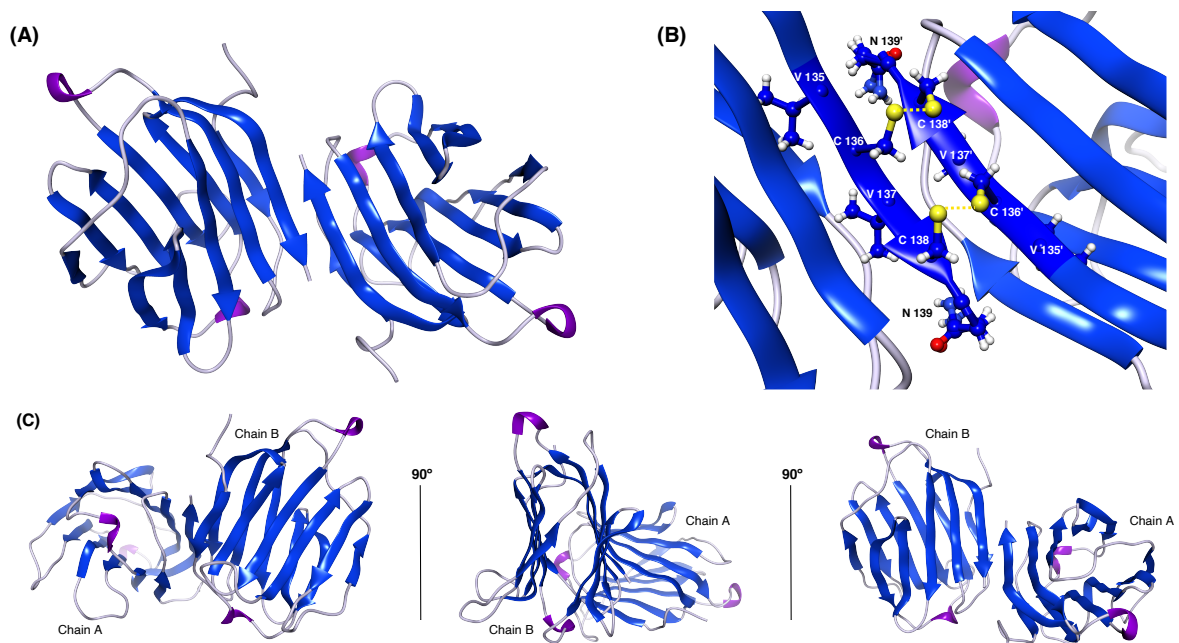
Expressed in epithelial cells of endometrium and trophoblasts, GAL-9 could play a role in immune regulation during all steps of the gestation (Meggyes *et al.*, 2014). Specific role of GAL-10 during pregnancy is still to be described, but low concentrations of this protein in maternal serum have been observed in spontaneous abortion patients, and its expression has been reported in syncytiotrophoblast and decidua during first trimester (Blois *et al.*, 2019). Dysregulation of GAL-13 expression was suggested to contribute to a dysregulation of immune responses required for a successful pregnancy outcome (Than *et al.*, 2014; Balogh *et al.*, 2019; Blois *et al.*, 2019). Functional features of this protein will be discussed in next section.

In summary, coordinated and simultaneous function of several galectins leads to a healthy pregnancy, because they are influencing immune adaptation, placental development, and angiogenesis.

Galectin-13 and its biological role

GAL-13 is classified as a prototype galectin, because in solution two identical subunits of 16 kDa form homodimers. GAL-13 is the only prototypic member of family whose CRD are associated through covalent interactions. In 1983, when Bohn and collaborators isolated this protein, they found out that dimerization involves disulfide bridges, but dimer interface was not described until 2018 when Su and coworkers solved GAL-13 structure by X-ray crystallography (Figure 6). Two disulfide bridges between C136 and C138 of each protomer along with hydrogen bonds between V135, V137 and N139, form dimer interface of GAL-13, which is located at amino terminus (Bohn, Kraus and Winckler, 1983; Than *et al.*, 2004; Su, Wang, *et al.*, 2018).

Figure 6. Galectin-13 homodimer (5XG7).



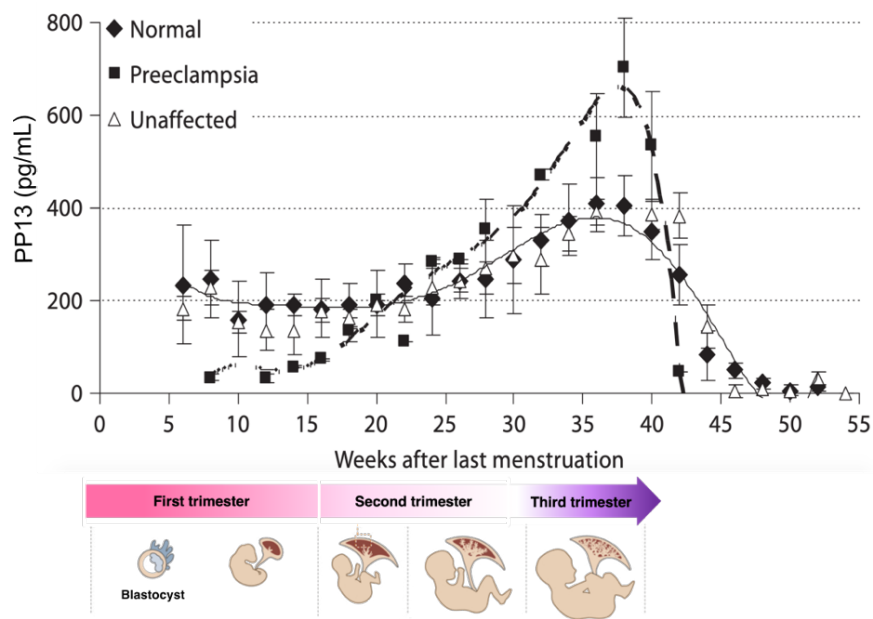
(A) Overall homodimer arrangement. (B) Dimer interface: two Cys residues (136 and 138) of each protomer form a pair of disulfide bridges. In addition, amide bond of residues V135, V137 and N139 form six hydrogen bonds. (C) Different projections of GAL-13 structure. Its architecture consists of a twisted side-to-side dimer.

GAL-13 is also known as Placental Protein 13 (PP13) because it was isolated from human placenta (Bohn, Kraus and Winckler, 1983). Placenta provides an immunological barrier between the mother and fetus, it mediates transfer of nutrients, water, gases and it sustains fetal growth by secreting hormones, cytokines, and signaling factors (Goldstein *et al.*, 2020). Thus, GAL-13 might be crucial for a successful pregnancy and fetal development outcome by being directly involved in placenta development and function (Sammar *et al.*, 2019).

GAL-13, along with other family members, is encoded on human chromosome 19q13.2. Together with galectins -14 and -16, GAL-13 is expressed in placenta, mainly at the syncytiotrophoblast. Through *in situ* mRNA hybridization, GAL13 was

also detected in amnion (fetal membrane) and extra villous trophoblast (invasive trophoblast) as well as fetal endothelial cells (capillary) (Than *et al.*, 2009). This protein is only expressed temporarily during pregnancy, at postpartum it disappears from mother's blood stream (Huppertz *et al.*, 2008). Maternal serum GAL-13 (PP13) concentration increases during normal pregnancy with a peak in third trimester (Figure 7). It is higher in patients with early pre-eclampsia compared to those with healthy pregnancies, however staining does not show significant differences in placenta from normal and preeclamptic pregnancies. Abnormal expression profiles of GAL-13 is associated with different obstetrical syndromes, such as miscarriage, pre-eclampsia and gestational diabetes mellitus (Table 3) (Than *et al.*, 2014; Vokalova *et al.*, 2020).

Figure 7. GAL13 (PP13) maternal serum concentration during pregnancy.



A correlation with fetal-placental unit development is shown. Graph in upper panel was taken from (Huppertz *et al.*, 2008), maternal serum concentration of GAL-13 (PP13) were different between healthy pregnancies (“Normal”), and those with pre-eclampsia or other complications (“Unaffected”). Scheme in lower panel was modified from Human Placenta Project, 2017 (available in <https://nichd.nih.gov>).

Table 3. Diseases during pregnancy with atypical concentration of GAL-13.

Obstetrical syndrome	GAL-13 expression*	Detection of GAL-13	Reference
Pre-eclampsia	Abnormal pattern	Maternal serum.	(Huppertz <i>et al.</i> , 2008)
	Truncated isoform	110 aa	
HELLP	Abnormal pattern	Syncytiotrophoblast membrane	(Balogh <i>et al.</i> , 2011)
Miscarriage	Decreased	Syncytiotrophoblast	(Balogh <i>et al.</i> , 2019)
Gestational Diabetes mellitus	Decreased	Syncytiotrophoblast and syncytiotrophoblast nuclei, trophoblasts and extra villous trophoblast. Maternal serum.	(Unverdorben <i>et al.</i> , 2015)
Preterm labor	Truncated isoform	101 aa, genomic DNA of whole maternal blood.	(Gebhardt, Bruiners and Hillermann, 2009)

* In comparison with expression profile in healthy pregnancies.

Early studies of GAL-13 interaction over-cultured trophoblasts showed it plays a role in placentation. GAL-13 (PP13), recombinant and directly isolated from placenta, caused calcium depolarization in trophoblasts (Burger *et al.*, 2004), which is essential for successful fetal development (Niger, Malassine and Cronier, 2004).

GAL-13 is exported from syncytiotrophoblasts as follows: it is colocalized with actin, then it interacts with annexin II, anchoring to lipid rafts at inner side of cellular membrane and finally, calcium ionophores induce formation and shedding of syncytiotrophoblast derived micro vesicles which are released into maternal circulation (Balogh *et al.*, 2011).

Animal models showed that GAL-13 have a relevant role in hemodynamics events characteristic of hemochorial placentation. Subcutaneous administration of 127 ng of GAL-13 (PP13) elicited reversible systemic hypotension (reduction of approximately 20% mean arterial pressure), induced fetal weight gain and it was associated with structural development of placental and uterine blood vessels

(Gizurarson *et al.*, 2016). A study of GAL-13 effect on female pregnant and non-pregnant rat's uterine arteria vasodilation showed that GAL-13 vasodilation occurs via eNOS and prostaglandin type 2 pathways (Drobnjak *et al.*, 2017), which might regulate blood flow between maternal and fetal-placenta unit.

GAL-13 interacts with immune system cells. Aggregates of GAL-13 have been found closer to zones of necrosis in maternal decidual veins containing T-cells, neutrophils and macrophages (Kliman *et al.*, 2012). There are data which allow to hypothesize that GAL-13 might lead immune cells towards a placental-growth-permissive environment by inducing polarization of neutrophils, and apoptosis of T-cells isolated from pregnant and non-pregnant women (Than *et al.*, 2009; Vokalova *et al.*, 2020).

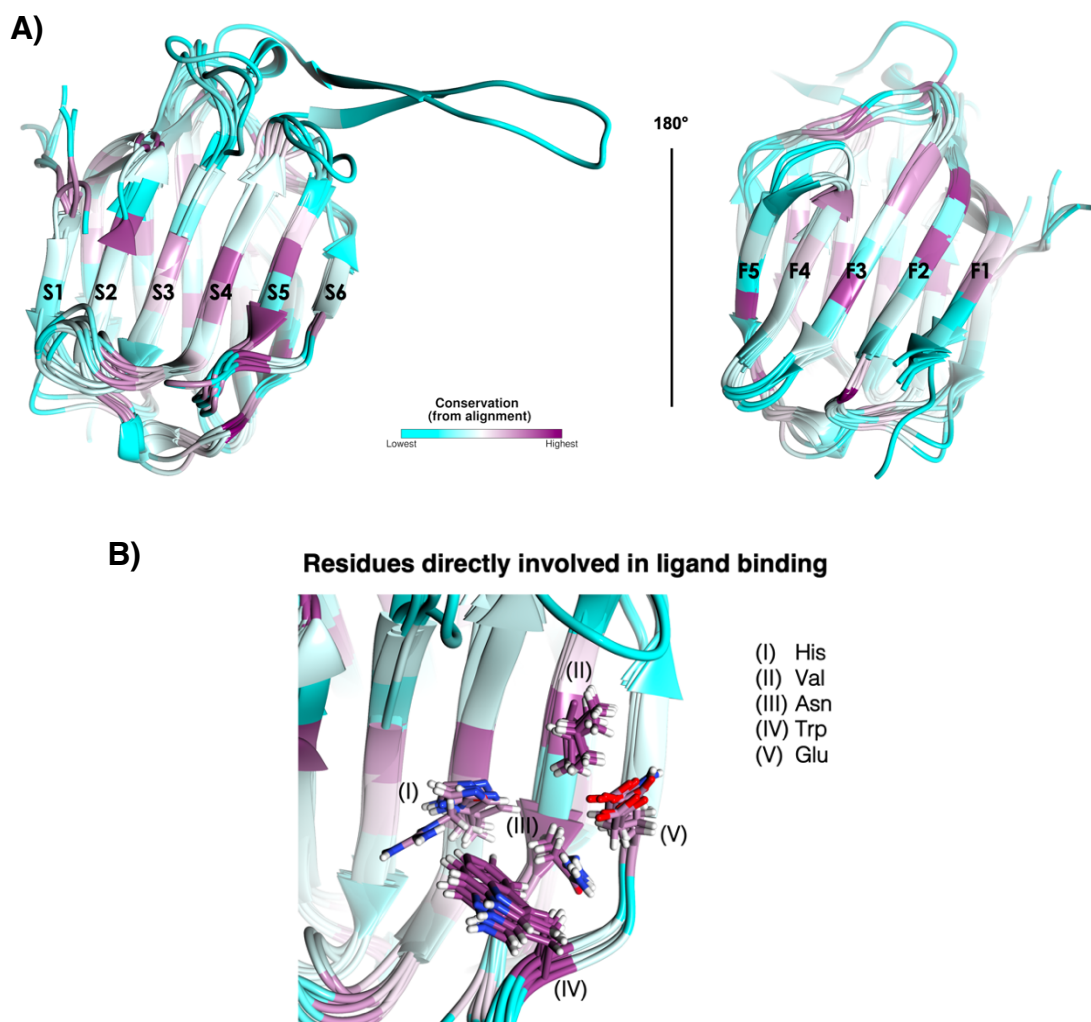
RESEARCH PROJECT

Problem statement

GAL-13 mechanism of action at molecular level remains to be studied. This is crucial for design of routes to boost prognosis and treatment of related diseases. The biological roles of GAL-13 are expected to rely on its glycan binding ability. As mentioned before, most galectins interact with β -galactosides. Highly conserved residues at GBS are directly involved in binding, as we confirmed by performing an alignment from structure overlay of human prototype galectins (GAL-1, -2, -7, -10, -13, -14 and -16) with UCSF Chimera (Figure 8).

There is a pattern in variability of residues lining the GBS between tissue localization of galectins. Galectins -13, -14 and -16, which are expressed in the placental trophoblasts, share more residues between themselves relative to GAL-1, -2 and -7, which are expressed in endothelium, and with GAL-10, which is primarily expressed in eosinophils. We expect this sequence variability to be linked with the molecular function of glycan binding and the tissue function of these galectins.

Figure 8. Conserved residues in CRD of human prototype galectins.



Structurally conserved residues of human prototype galectins: -1 (1GZW), 02 (5DG1), -7 (4GAL), -10 (1LCL), -13 (5XG7), -14 (6K2Y) and -16 (6LJP) are colored in magenta and non-conserved residues are colored in cyan (A). GBS zoom is shown to highlight key residues for ligand recognition (B). Residues (I) His is an Arg in GAL-13, and (V) Glu is a Gln in GAL-10.

Within a functional study, Than and coworkers concluded that GAL-13 prefers to bind carbohydrates with aminated moieties over regular sugars. Through a chromatographic-like approach, the authors reported that GAL-13 (PP13) exhibited

affinity (in decreasing order) towards N-acetyl lactosamine (LacNAc), D-mannose, N-acetyl galactosamine, D-maltose, D-glucose, D-galactose, D-fucose and α -D-lactose (Than *et al.*, 2004).

However, in recent years, Mayo and collaborators concluded that GAL-13 probably does not bind carbohydrates because replacement of a histidine residue to an arginine at position 53, and an arginine to a histidine at position 57, may interfere with ligand recognition and binding (Su, Cui, *et al.*, 2018; Yang *et al.*, 2020). Indeed, they also reported GBS independent functions of GAL-13. Thus, true importance of GAL-13 residues within its GBS for biological processes associated to the protein, including those identified during pregnancy, is still under debate.

Hypothesis and Objectives

Our research hypothesis is that conserved residues in the GBS are necessary for GAL-13 function.

During pregnancy, GAL-13 plays a role in placentation and placental angiogenesis (Sammar *et al.*, 2019). As member of galectin family, it has been proposed that these cellular functions occur via interactions of GAL-13 and glycosylated moieties of extracellular matrix at maternal-fetal interface. However, contradictory data found by different research groups while trying to characterize glycan binding, highlights the importance of understanding whether conserved residues in the GBS are necessary for GAL-13 function. By construction of mutants at conserved residues in the GBS of GAL-13 their role in function could be assessed.

This study aims to develop and put in place methodologies to characterize physicochemical properties and activity of GAL-13 that will form the basis to set up experimental conditions which will allow answering this proposed hypothesis.

Specific objectives

- 1) Expression and purification of recombinant GAL-13.
- 2) *In vitro* characterization of recombinant GAL-13 by physicochemical probes and activity assays with placental choriocarcinoma cell line and rat aortas.
- 3) Determination of dissociation constant values (K_D) of GAL-13 and aminated glycans.
- 4) Design and preparation of GBS point mutants of GAL-13.

METHODOLOGY

1) Expression and purification of GAL-13

Over-expression

a) Genetic construct of GAL-13

The system used to over-express and produce wild-type (wt) recombinant GAL-13 and mutants was *Escherichia coli* BL21 (DE3). wt-GAL-13 over expression construct within a pET-22b (+) vector was synthesized by Biobasic®, codons were optimized for expression in *E. coli*.

b) Construction of GAL-13 point mutants

Plasmid of wt-GAL-13 was used as site-directed mutagenesis template. Primer design was performed by using NEBaseChanger™ tool from New England BioLabs®, available online (nebasechanger.neb.com) and mutants were synthesized by AlphaDNA (Montreal, QC, Canada). Mutagenesis was carried out by using New England BioLabs® Inc. Q5® site directed mutagenesis kit. Mutation constructions were confirmed by DNA sequencing service, performed at the Centre d'expertise et de services Génome Québec (Montréal, Canada).

Table 4. Primers used for mutagenesis.

Mutant		Primer Sequence	Length	T _m (°C)	GC (%)
R53A	F	5' CATCGCGTTTCGCGTTCCGTGTTTAC 3'	25	58	60
	R	5'TCAGAGTCTTCGTCCATG 3'	18	60	50
R55A	F	5'GTTCCGTTTCcgcGTTCACTTCGGTAAC 3'	23	64	56.5
	R	5'GCGATGTCAGAGTCTTCG 3'	18	62	55.6
H57A	F	5'TTTCCGTGTTGCGTTCGGTAACCACGTTGTTATG3'	34	62	47.1
	R	5' CGGAACGCGATGTCAGAG 3'	18	65	61.1
V63A	F	5'TAACCACGTTGCGATGAACCGTC3'	23	59	52.2
	R	5'CCGAAGTGAACACGGAAAC3'	18	63	50
N65A	F	5' CGTTGTTATGGCGCGTCGTGAATTTGG 3'	27	58	51.9
	R	5'TGGTTACCGAAGTGAACAC3'	19	62	47.4
E75A	F	5' CTGGATGCTGGCGGAAACCACCG 3'	23	62	65.2
	R	5' ATGCCAAATTCACGACGG 3'	18	63	50

c) Over-expression procedure

Competent cells are transformed by electroporation with the plasmid containing the coding sequence for GAL-13. In order to produce recombinant wt-GAL-13 and mutants, an overnight starting culture of liquid LB media with transformed cells is scaled to 1L of MJ medium, and it is incubated at 37 °C until it reaches A₆₀₀ of 0.6. Induction of GAL-13 over-expression is performed by addition of isopropyl β-D-thiogalacto pyranoside (IPTG) (final concentration of 0.2 mM) to culture. Then, incubation temperature is decreased to 16 °C and cells are incubated overnight (O/N). Cells are isolated from culture media by centrifugation for 30 min at 4 °C and 5,000 rpm. Presence of protein with expected molecular weight for GAL-13 both in soluble fraction and within inclusion bodies of harvested cells was confirmed by SDS-PAGE (see below).

MJ minimal medium allows control of both carbon and nitrogen sources, which consists of a mixture of: MEM vitamin solution, metal solution (50 mM FeCl₃ · 6H₂O,

20 mM $\text{CaCl}_2 \cdot 6\text{H}_2\text{O}$, 10 mM MnSO_4 , 20 mM ZnCl_2 , 2 mM of $\text{CoCl}_2 \cdot 6\text{H}_2\text{O}$, $\text{CuSO}_4 \cdot 5\text{H}_2\text{O}$, $\text{NiSO}_4 \cdot 6\text{H}_2\text{O}$ and H_3BO_3 , 20 % (w/v) glucose up to final concentration 2 mM, 7.5 mM MgSO_4 , $50 \mu\text{g mL}^{-1}$ Ampicillin, $70 \mu\text{g mL}^{-1}$ Thiamine dissolved in base MJ medium (100 mM phosphates buffer pH 6.6 with 45 mM NH_4Cl and sodium citrate dihydrate).

Purification

First step to purify recombinant GAL-13, wild type and mutants, consisted of cell lysis of resuspended cells by sonication. Pellet of harvested cells was resuspended in purification buffer: 20 mM TRIS buffer with 100 mM NaCl and 1 mM 2-mercaptoethanol at pH 8.7. Soluble protein extract was obtained by centrifugation of total lysate at 15,000 rpm and 4 °C for 30 min.

Second step to purify GAL-13, wild type and mutants, consists of salting out. GAL-13 enriched pellet is precipitated by addition of ammonium sulfate up to 38 % of saturation for the volume of protein solution at 4 °C (calculated with the relationship in Supplementary Information 13, section A.3 F.1 of (Hermodson, 1996), for wt-GAL-13 and V63A-GAL-13). Purification of N65A-GAL-13 was improved when lysate was salted out to 41 % of $(\text{NH}_4)_2\text{SO}_4$ saturation. Precipitated protein pellet enriched with GAL13 was collected by centrifuging salted out solution at 10,000 g and 4 °C for 15 min.

Before moving to chromatographic purification, $(\text{NH}_4)_2\text{SO}_4$ excess was removed. Thus, salted out precipitate was resolubilized in less than 10 mL of 20 mM phosphate buffer pH 8.7 with 100 mM NaCl. Dialysis was then performed at 4 °C

against 4L (6X) of purification buffer (20 mM TRIS at pH 8.7 with 100 mM NaCl, and 1 mM 2-mercaptoethanol).

Third step consists of a size exclusion chromatography. Purification is performed with a GE ÄKTA FPLC™ equipped with a Superdex™ 75 10/300 column, previously equilibrated with purification buffer (TRIS 20 mM at pH 8.7 with 100 mM NaCl, 1mM 2-mercaptoethanol). wt-GAL-13 and mutants elute at approximately 17 min by using a flow rate of 0.5 mL min⁻¹. Purified wt-GAL-13 and mutants is quantified using Beer-Lambert's equation with a GAL-13 extinction coefficient of 16,180 M⁻¹cm⁻¹, as calculated from GAL-13 amino acid sequence using ProtParam tool developed by Swiss Institute of Bioinformatics, available on ExPASy resource portal (Gasteiger *et al.*, 2005). An identical value was used for mutants.

2) Characterization of GAL-13

Protein Sequencing

Tandem mass spectrometry (MS/MS) data collection and analysis were carried out by Center for Advanced Proteomic and Chemogenomic Analyses (CAPCA, Montreal, QC, Canada). All MS/MS samples are analyzed using PEAKS studio from Bioinformatics Solutions (Waterloo, ON Canada) version 10.5 (2019-11-20). PEAKS studio is set up to assume trypsin digestion, and then to search the Uniprot_swissprot_human_JUN08_2018 data base, with a fragment ion mass tolerance of 0.30 Da and a parent ion tolerance of 10.0 ppm.

Protein identification was performed by using Scaffold (version 4.11.1) from Proteome Software Inc. (Portland, OR, USA) to validate MS/MS-based peptide and

protein identifications. Protein identifications were accepted if they could be established at greater than 97.0 % probability to achieve an FDR less than 1.0 % by the Scaffold Local FDR algorithm. Protein identifications were accepted if they could be established at greater than 71.0 % probability and contained at least 1 identified peptide. Protein probabilities were assigned by the Protein Prophet algorithm (Nesvizhskii *et al.*, 2003). Proteins that contained similar peptides and could not be differentiated based on MS/MS analysis alone were grouped to satisfy the principles of parsimony.

SDS-PAGE and Western Blot

All SDS-PAGE samples were prepared by boiling protein samples in Laemmli buffer, 250 mM TRIS-HCl at pH 6.8 with 40 % glycerol (v/v), 2 % SDS (w/v), 20 % 2-mercapto ethanol (v/v), 0.01 % bromophenol blue (w/v). Proteins samples were migrated on Mini-PROTEAN® TGX™ 4-20 % pre-cast gels (BioRad Laboratories) at constant voltage until Laemmli dye front reached the bottom of the gel.

Separated proteins were transferred onto a PVDF membrane at 100 V and at 5 °C for 1h by using a Mini-PROTEAN II system (BioRad Laboratories) and 25 mM TRIS-base with 192 mM Glycine and 20 % (v/v) methanol, membrane was blocked for 1h with 3 % (w/v) of bovine serum albumin (BSA) in 1 × TBS, 15 mM TRIS-HCl pH 7.6 with 130 mM NaCl. After washing three times with 1 × TBST, 15 mM TRIS-HCl pH 7.6 with 130 mM NaCl and 0.05 % (v/v) Tween 20, membranes were incubated 16h at 4°C with primary antibody (1:2,000), diluted in TBST with 1 % (w/v) BSA and 0.05% (w/v) NaN₃, followed by another incubation at room temperature 1h with secondary antibody (1:10,000), diluted in TBST with 3 % (w/v) BSA. Membrane was revealed by adding UltraScience Pico Ultra Western Substrate from FroggBio

(Toronto, ON, Canada) to generate a chemiluminescent response in presence of the HRP-conjugated secondary antibody.

Galectin-13 antibody LS-C179128 (primary antibody) was obtained from LSBio (Seattle, WA, USA). It is an unconjugated rabbit polyclonal antibody to human galectin-13 (LGALS13). Secondary antibody was goat anti-rabbit HRP-conjugated antibody (Invitrogen-Thermofischer Canada, Ottawa, ON, Canada).

Semi native SDS-PAGE

GAL-13 aliquot was dialyzed against 20 mM phosphates buffer pH 7.5 with 100 mM NaCl, and split in half. Then 1 mM of 2-mercapto ethanol was added to just one of the portions of protein solution. Dilution series were prepared with increasing concentrations of GAL-13, ranging from 2 – 24 μ M, and loaded onto a Mini-PROTEAN® TGX™ 4 – 20 % pre-cast gels (BioRad Laboratories) and migrated as described previously. Samples were prepared as described above for denaturant gel electrophoresis, with the only difference being that loading buffer did not contain 2-mercapto ethanol.

Mass Spectrometry

Mass determination of GAL-13, wild type and mutants, was assessed with a Bruker Daltonics Microflex system which uses MALDI-TOF/TOF ionization. Data acquisition was performed in linear mode, by using a 337nm laser with ion source and lens voltages set at 19.44 kV and 7.04 kV, respectively. Samples with recombinant protein were diluted and mixed with α -cyano-4-hydroxycinnamic acid matrix.

Circular dichroism (CD)

Secondary and tertiary structure of GAL-13, wild type and mutants, was evaluated by collecting CD spectrum of far and near UV, respectively. All CD monitored experiments were performed using a JASCO J815 CD spectropolarimeter and 1 mm path length quartz cuvettes. Samples contained GAL-13 (concentration ranging from 20 to 70 μM) diluted in purification buffer, TRIS 20 mM at pH 8.7 with sodium chloride 100 mM, previously filtered at 0.2 μM . Far UV spectra were collected with 9 accumulations from 260 to 190 nm. Near UV spectra were collected from 300 to 260 nm. Spectroscopic data analysis and plots were performed with GraphPad Prism v.9.2.0. Molar ellipticity, $[\theta]$, for all CD spectra was calculated as follow:

$$[\theta] = \frac{100 \cdot \theta}{l \cdot c} \text{ (deg cm}^2 \text{ dmol}^{-1}\text{)}$$

Where θ is ellipticity at each given wavelength of spectrum, l is path length (cm) and c is molar protein concentration.

Thermal unfolding experiments were performed by measuring changes in ellipticity of GAL-13, wild type and mutants, at 220 nm (greatest signal observed in far UV spectra) upon increasing temperature with a rate of 1 $^{\circ}\text{C min}^{-1}$, from 10 up to 100 $^{\circ}\text{C}$.

Activity assays

a) Cell proliferation assay

Cell culture: JEG-3 cells from the American Type Culture Collection (ATCC, Rockville, MD) were kindly provided by prof. Cathy Vaillancourt (INRS-Centre Armand-Frappier Santé Biotechnologie, Laval, QC, Canada). Cells were maintained in minimum essential medium (MEM) Eagle (Sigma-Aldrich, Oakville, ON, Canada) supplemented with 1.1 g mL⁻¹ sodium bicarbonate, 1 mM sodium pyruvate, 0.01 mM HEPES (Sigma-Aldrich) and 10% fetal bovine serum (FBS, Wisent Bioproducts, St-Bruno, QC, Canada). Cells were cultured within 75 cm² flasks (from Sarstedt AG & Co. KG, Nümbrecht, Germany), in a humidified atmosphere with 5 % carbon dioxide (CO₂) at 37 °C. Cells were passaged when they reached about 70 % confluence using 0.5 % trypsin (GIBCO, Life Technologies corporation, Grand Island, NY, USA).

Cell proliferation: JEG-3 cells (1.5 × 10⁵ cells mL⁻¹) were seeded into 96-well cell culture plates (Thermo Scientific Nunc® Rochester, NY, USA) in their complete culture medium and were allowed to climatize for 24 h incubation. Then, culture medium was exchanged to serum free medium (MEM supplemented with 1.1 g mL⁻¹ sodium bicarbonate, 1 mM sodium pyruvate and 0.01 mM HEPES), and after a 6h incubation, cells were treated with increasing concentrations of GAL-13 from 10⁻¹¹ to 10⁻⁶ M. Before each set of experiments, all protein samples were dialyzed (6X) against 4L phosphates buffer 20 mM pH 7.5 with 100 mM of NaCl, to remove any trace of purification buffer, 2-mercapto ethanol and/or ammonium sulfate.

After 72 h of incubation, resazurin reagent (CellTiter Blue, ThermoFischer Scientific Canada, Ottawa, ON, Canada) was added to wells following protocol described by the supplier. Fluorescence of each well was read (560λ_{ex}/590λ_{em} nm) using an infinite M1000 microplate reader (from TECAN Trading AG, Switzerland), once cells had been incubated for 2.5 - 3h with resazurin reagent.

Experiments were performed as five biological replicates, each performed with 3 technical replicated. Statistical analyses and figures were made using GraphPad Prism v.9.2.0 (GraphPad Software, San Diego, CA) with one-way ANOVA test to assess significant differences. A value of $P < 0.05$ was considered statistically significant.

b) Vasodilatation assay

Thoracic aortas (aortic arch to diaphragm) from male Sprague-Dawley rats of 200-250 g (7 to 8 weeks old) were placed in Krebs-Heinselet solution (118 mM NaCl, 4.7 mM KCl, 2.5 mM CaCl_2 , 1.2 mM KH_2PO_4 , 1.2 mM MgSO_4 , 25 mM NaHCO_3 , 11 mM glucose), cleaned of surrounding adipose and connective tissues, and cut in 3 - 4 mm long segments. Then aorta rings were carefully mounted in 5 ml organ baths filled with Krebs-Heinselet buffer aerated with a 95 % O_2 / 5 % CO_2 gas mixture and maintained at 37 °C. Rings were allowed to equilibrate for 1h under a 1g initial tension with buffer changes every 15 min before data recording. Isometric force-displacement transducers connected to a Grass 7E polygraph (Grass Instruments, Gainesville, FL, USA) was used to collect data. Integrity of aortic rings (smooth muscle and endothelial cell layers) was verified by contraction under 30 mM KCl followed by relaxation induced with 10^{-5} M acetylcholine. Dilation of dissected tissue was observed after addition of wt-GAL-13 to previously contracted aortas with 30 mM potassium chloride. Relative response percentages for each wt-GAL-13 concentration were calculated considering the ratio of dilation induced by acetylcholine over the 30 mM contraction as 100 % response. Results were depicted using GraphPad Prism v.9.2.0 and represent data collected from aortic rings from 5 different animals.

Before each set of experiments, all GAL-13 samples were dialyzed (6X) against 4L phosphates buffer 20 mM pH 7.5 with 100 mM of NaCl, to remove any trace of purification buffer, 2-mercapto ethanol and/or ammonium sulfate.

3) Binding assays with GAL-13

Fluorescence assay

This experiment was set-up to assess GAL-13 binding to several mono and disaccharides. Emission profile of all samples was measured with an infinite M1000 microplate reader (from TECAN Trading AG, Switzerland). Fluorescence spectra of dilution series were collected from 315 to 400 nm, and to selectively excite W72^{hGAL13} in GBS, a wave length of 295 nm was used. Each dilution contained GAL-13 [50 μ M] with ligand to test at increasing concentrations from 0 to 20 molar equivalents. Binding was determined by evaluating changes in center of mass (COM) of each fluorescence spectra upon titration with ligand. COM is calculated as follow:

$$\text{COM} = \frac{\sum_{i=0}^n \lambda_i I_i}{\sum_{i=0}^n I_i}$$

Where λ and I are, respectively, the wavelength and intensity for each point (i) of the spectrum. Then, a plot of concentration of ligand against COM of fluorescence spectra was constructed. Plots were depicted using GraphPad Prism v.9.2.0.

Isothermal Titration Calorimetry (ITC)

To determine dissociation constant values of disaccharides binding to GAL13, ITC experiments were performed at room temperature (20 °C approximately) using a

NanoITC-LV instrument from TA Instruments – Waters LLC company (New Castle, DE, USA). Injections of 1.94 μL of 100 mM N-acetyl lactosamine (LacNAc) were added from a computer-controlled syringe at intervals of 150 s into the sample solution of 100 μM GAL-13 (cell volume = 350 μL) with stirring set at 310 rpm. Data collection and system control was set by using ITC run software; and fit of experimental data to a titration curve with determination of K_a/K_D as well as thermodynamic parameters of binding reaction were calculated by using NanoAnalyze software; both programs are supplied by TA Instruments – Waters LLC (New Castle). Raw data was extracted to prepare plots using GraphPad Prism v.9.2.0.

Microscale Thermophoresis (MST)

MST experiments were performed by using a Monolith NT.115Pico instrument (Nano Temper Technologies, Munich, Germany) using MO.Control and MO.Analysis (v1.6.1) software from Nano Temper Technologies to achieve data collection and analysis, respectively. Figures were made using GraphPad Prism v.9.2.0. Labeling of GAL-13 was carried out following the protocol for N-hydroxy succinimide (NHS) coupling of RED-NHS second generation dye (MO-L011; Nano Temper Technologies) to lysine (K) residues. Binding tests were performed using regular Monolith NT.115 capillaries under 20 % LED power, 10 nM label-GAL-13 was titrated with 400 μM ASF by preparing dilution series with increasing concentrations of ASF up to 200 mM and final GAL-13 concentration of 5 nM.

Assay and ligand (ASF) solubilization buffer composition were 100 mM TRIS at pH 8.0 with 200 mM MgCl₂ and 0.1% (w/v) PEG4000.

ELISA

Binding towards ASF was also probed using enzyme-linked immunosorbent assay (ELISA). Therefore, a Nunc MaxiSorp™ 96-well plate (Thermofischer, Rochester, NY, USA) was coated O/N at 4°C with ASF to a final concentration of 10 ng mL⁻¹. After an O/N blockage, carried out by using 10 % BSA in PBST (phosphate buffered saline with Tween, 3.2 mM Na₂HPO₄, 0.5 mM KH₂PO₄, 1.3 mM KCl and 135 mM NaCl with 0.05 % v/v Tween 20 at pH 7.4), dilution series of GAL-13, wild type and mutants, were added in each well up to a final concentration ranging from 1 nM to 1 μM. Then, the plate was incubated for 1h with a 1:5,000 galectin-13 antibody LS-C179128 (primary antibody, LSBio Seeattle, WA, USA) dilution prepared in PBST with 1 % (w/v) BSA. Then plate was washed three times with PBS before adding anti-rabbit HRP-conjugated antibody (secondary antibody, 1:10,000) for another 1h incubation. Immune recognition reaction was detected by using 3,3',5,5'-tetramethylbenzidine as substrate of HRP. Mean values of replicates were used to depict graphs which were also constructed with GraphPad Prism v.9.2.0.

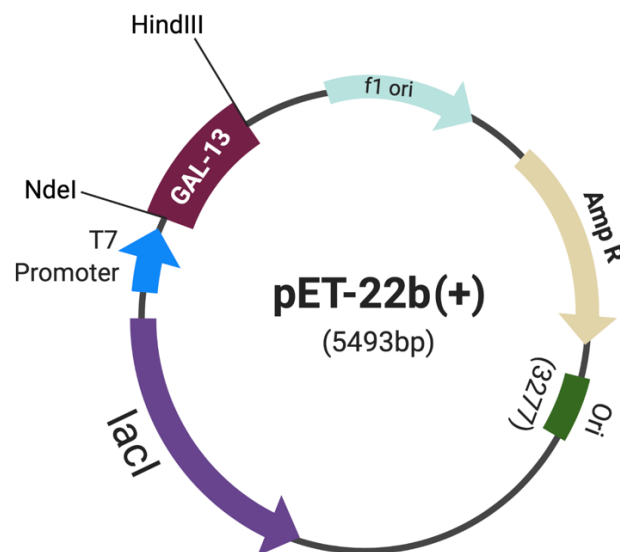
RESULTS AND DISCUSSION

1) Recombinant GAL-13 production and Purification

1.1) Over-expression

The system used to over-express and produce recombinant GAL-13 was *Escherichia coli* (see strains below) with a pET-22b (+) vector that contains GAL-13 gene with codons optimized for expression in this species (Figure 9). In this expression system, production of the encoded protein is triggered by IPTG, an analogue of lactose. Indeed, the *lacO* operon is regulated by a T7 promoter: when IPTG binds to the *LacI* repressor bound to the promoter region of the plasmid, then the T7 RNA polymerase of T7 bacteriophage encoded on the DE3 episome from the *E. coli* bacteria can start transcription of the encoded GAL-13 gene.

Figure 9. Plasmid map of vector pET-22b (+).



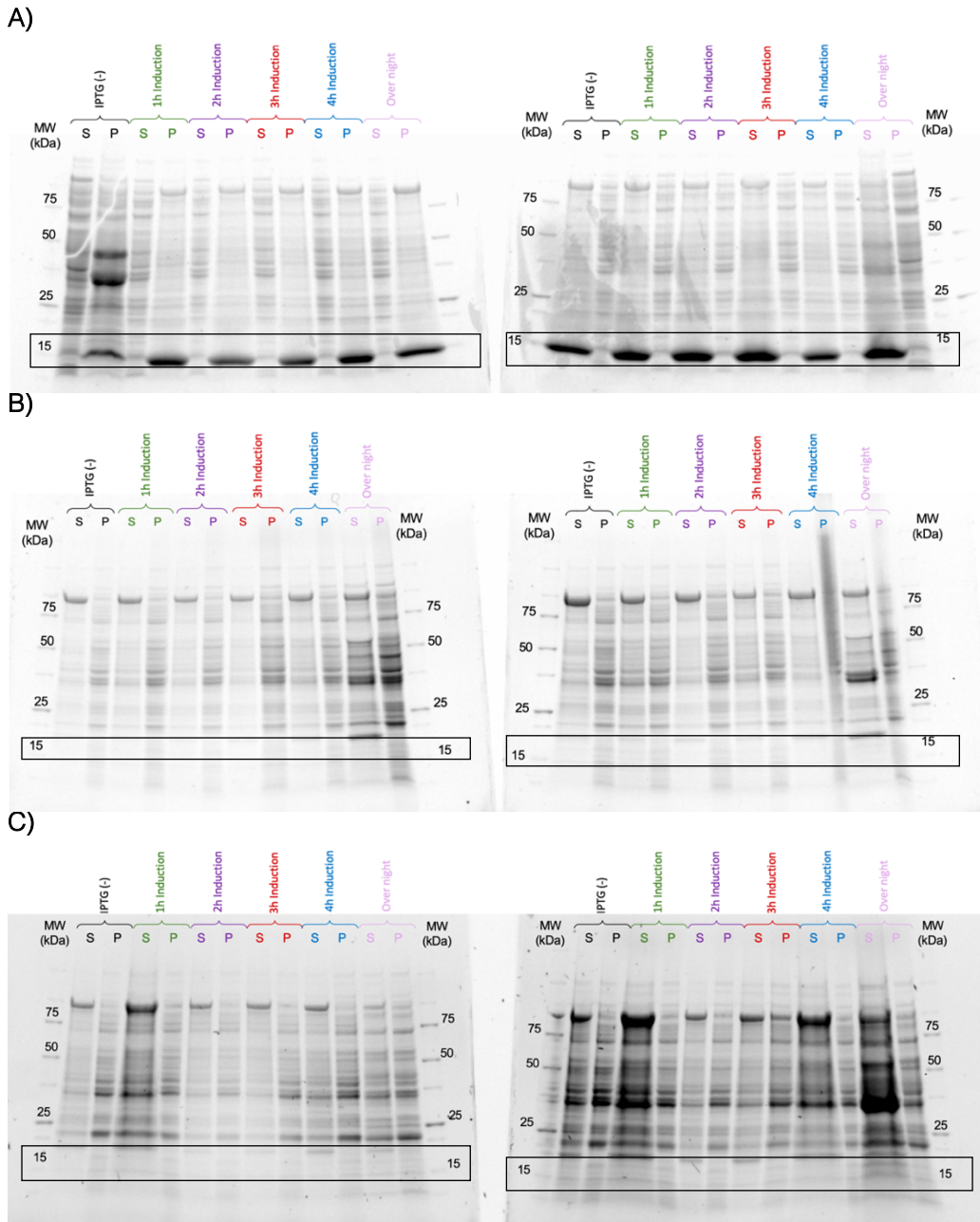
GAL-13 coding sequence is flanked by NdeI and HindIII restriction sites. Modified from Novagen (www.emdmilipore.com).

To assess proper over-expression conditions of our recombinant protein, we performed preliminary assays to verify induction and over-expression profile (Figure 10).

Three *E. coli* strains were tested: BL21 (DE3), Origami 2 (DE3) and Rosetta-Gami (DE3). Origami 2 (DE3) is used to facilitate proper disulfide bond formation, and Rosetta-gami (DE3) allows for enhanced disulfide bond formation and enhanced expression of eukaryotic proteins that contain codons rarely used in *E. coli*.

All three strains were transformed and over-expression profiles of recombinant protein were obtained from cultures grown at constant temperature (16 °C) with rich and starving medium, LB and MJ-minimal respectively. After IPTG addition, protein content was evaluated by SDS-PAGE hourly during the first 4 h of incubation and after 12 h incubation (overnight, O/N).

Figure 10. Evaluation of GAL-13 over-expression profiles in different *E. coli* strains.



(A) BL21 (DE3), (B) Origami-2 (DE3), and (C) Rosetta-Gami (DE3) at different incubation time. Figure shows a comparison between a LB and MJ-minimum medium, with gels on left and right side, respectively. Ladder labels were used to denote “soluble fraction” (S) and “insoluble fraction” (P).

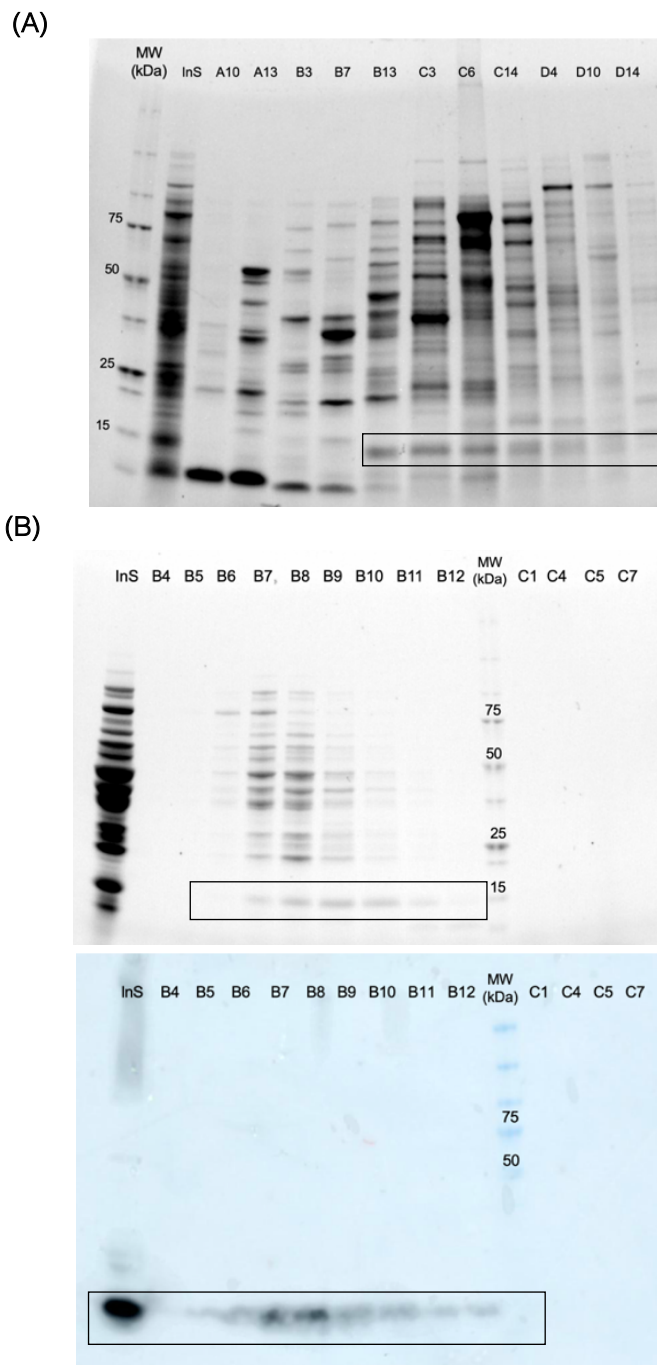
A protein band corresponding to the molecular weight of GAL-13 (16 kDa) was not observed in samples of Rosetta-Gami (DE3), while for Origami-2 (DE3) samples a faint band was observed. In contrast, thick bands were present in BL21 (DE3) samples. When expressing recombinant protein with strain BL21 (DE3) in minimal medium, the proportion of protein with molecular weight corresponding to GAL-13 is present mainly in the soluble fraction, in contrast to LB medium, where the protein is primarily expressed as inclusion bodies (insoluble fraction). In all cases, no significant change on induced cultures was observed with incubations between 1-4 h.

Through this preliminary test, it was shown that higher proportions of soluble recombinant GAL-13 protein are obtained when expressing in *E. coli* BL21 (DE3) and incubating cultures at 16 °C. Besides higher protein production yield, no significant difference in expression profiles was observed between 4 – 12 h. Therefore, we standardize induced cultures incubation for 12 h, in order to increase protein production yield.

1.2) Purification and Quantification

Chromatographic approach frequently used for galectin purification involves agarose beads modified with lactose, which is not feasible in our case as GAL-13 does not bind α -D-lactose. The isoelectric point of GAL-13 is 5.43, therefore, we first attempted to purify it through anion exchange chromatography, followed by size exclusion chromatography.

Figure 11. GAL-13 purification attempt through anion exchange and size exclusion chromatography.

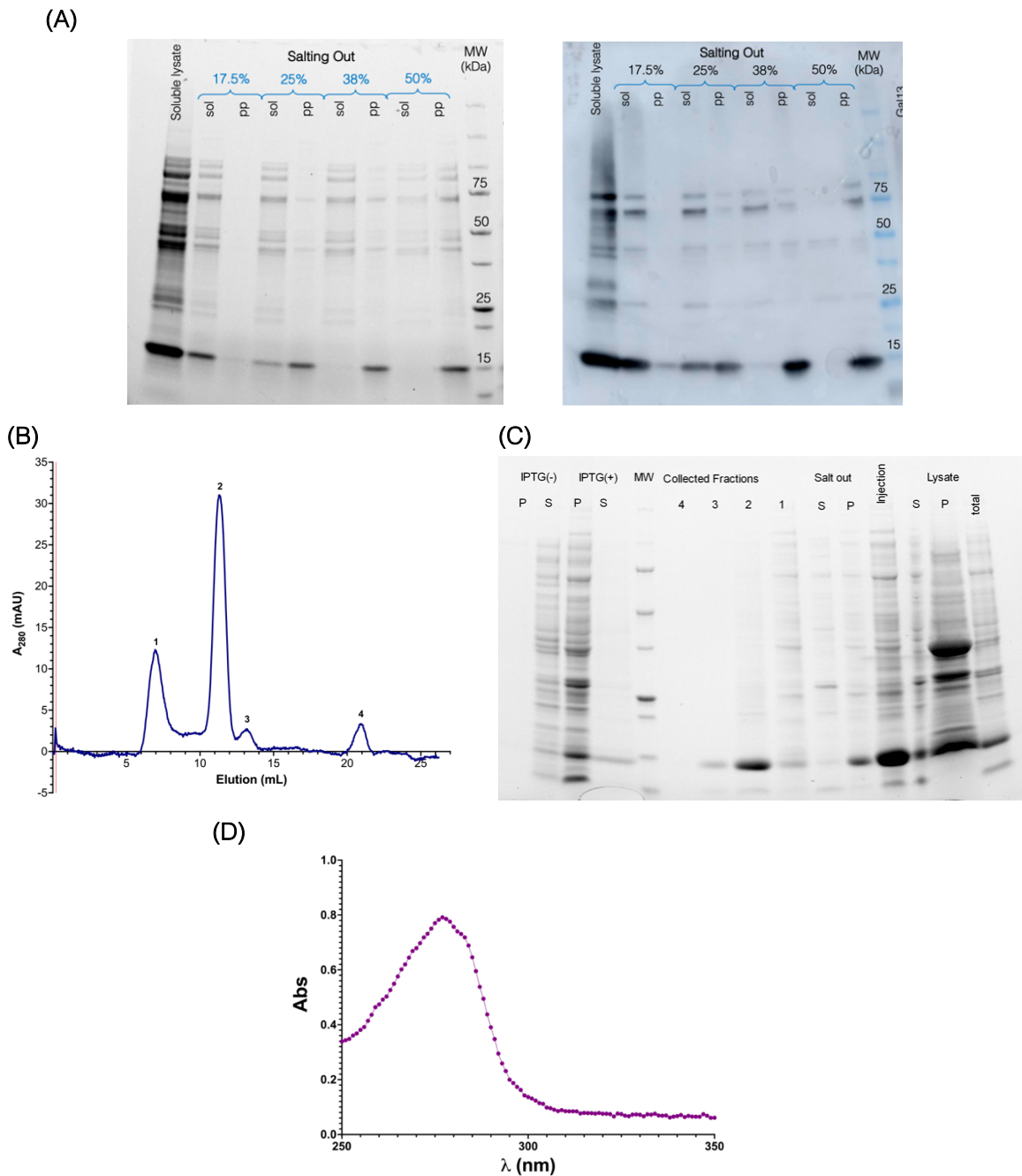


SDS-PAGE (left) analyses of fractions collected through (A) anion exchange chromatography carried out by using a HiTrapQ column with an elution profile following a linear gradient of 1M sodium chloride and (B) size exclusion chromatography (top gel), with western blot shown on the bottom gel. InS refers to injected sample and all other labels correspond to collected fraction numbers.

Through mentioned chromatographic approach, we expected to obtain a solution enriched with clean recombinant protein. However, after anion exchange step, recombinant protein coeluted with other proteins from which it could not be isolated in the next step, as confirmed by SDS-PAGE (Figure 11). Western blot analysis allowed us to conclude that the recombinant protein is over-expressed and recognized by commercial anti-human galectin-13 antibody.

The first procedure shows that protein content in clarified lysate and eluted fractions from anion and size exclusion chromatography were not significantly different. Therefore, to assess clarification of cell lysate, we performed a fractional precipitation prior to a chromatography purification. We salted out soluble lysate of over-expressed cells at 17.5, 25, 38 and 50 % of saturation with ammonium sulfate. Protein precipitate enriched with GAL-13 and fewer impurities was obtained at 38% of $(\text{NH}_4)_2\text{SO}_4$ (Figure 12-A). Salted out proteins containing GAL-13 were solubilized and purified by size exclusion chromatography, after dialysis against the purification buffer, to remove excess of ammonium sulfate (Figure 12, B and C).

Figure 12. Purification of GAL-13.



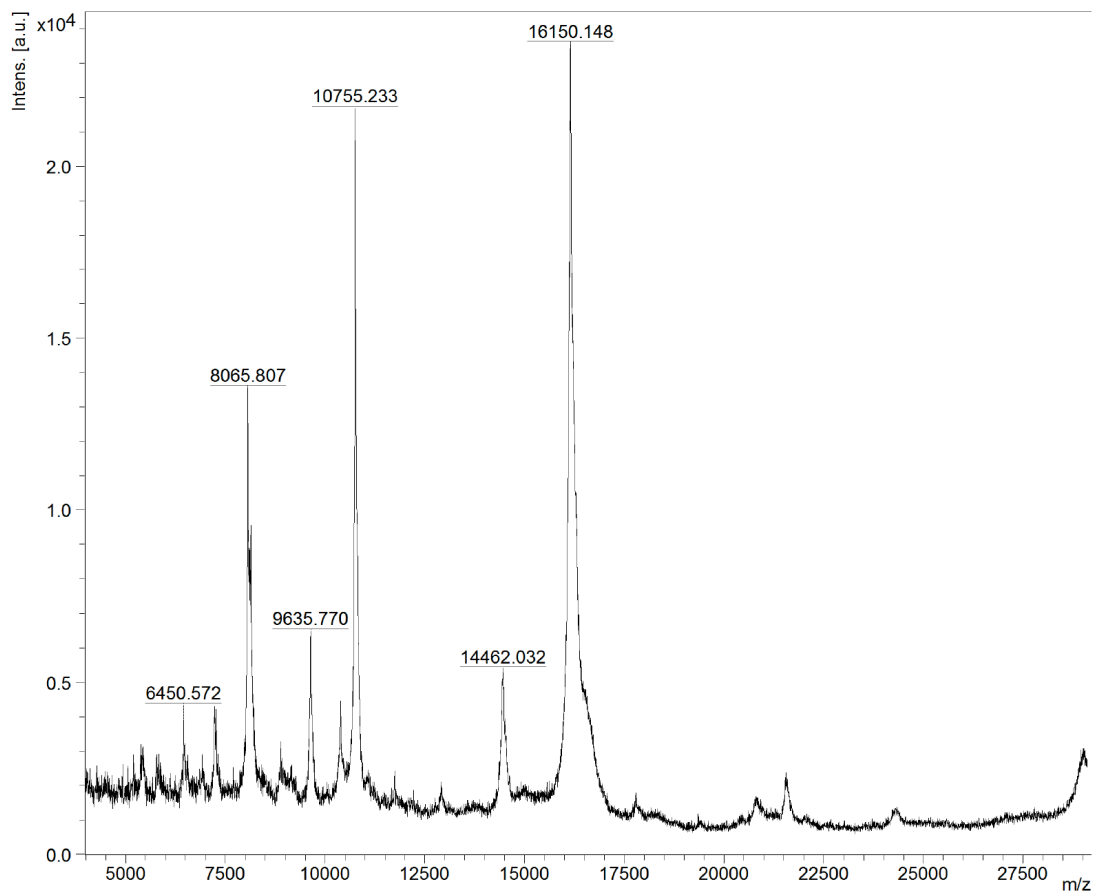
(A) SDS-PAGE, right panel, and WB, left panel, showing stepwise increase of ammonium sulfate concentration. (B) An example of size exclusion chromatogram, red line indicates injection, each peak with high absorbance is numbered. (C) SDS-PAGE verification of samples taken from over expression, salting out and SEC purification, labels “S” and “P” mean soluble and insoluble fractions, respectively, numbers of collected fractions correspond to observed peaks in chromatogram. (D) Example of GAL-13 UV-vis spectrum, collected to quantify protein.

We could standardize purification efficiency by performing two other purifications of GAL-13 over-expressed on independent batches. Quantification of GAL-13 is directly assessed from maximum of UV-vis spectrum using an extinction coefficient value of $16,180 \text{ M}^{-1} \text{ cm}^{-1}$ (Figure 12-D), as from GAL-13 amino acid sequence using ProtParam tool developed by Swiss Institute of Bioinformatics, available on ExPASy resource portal (Gasteiger *et al.*, 2005). On average, we obtain roughly 20 to 30 mL of GAL13 concentrated at 3.6 mg mL^{-1} .

To verify the molecular weight of the putatively purified GAL13, we performed mass spectrometry assays directly on the purified samples, Figure 13. The most abundant ionized species has a mass-charge ratio of 16,150.148 Da, which is 31.568 Da higher than GAL-13's molecular weight calculated from protein sequence (16,118. Da). Such difference between expected and observed molecular ion m/z can be mainly due to the average of isotopic contribution from all atoms composing the protein, which also broadens peaks, as well as to average exposed residues' side chains modifications occurring during ionization step (Hung *et al.*, 2007). A peak of approximately half of GAL-13 molecular weight was also observed (peak 8065.807 Da). Such signal is probably due to a protein ionization state of +2, resulting in a mass/charge peak at half of the expected MW.

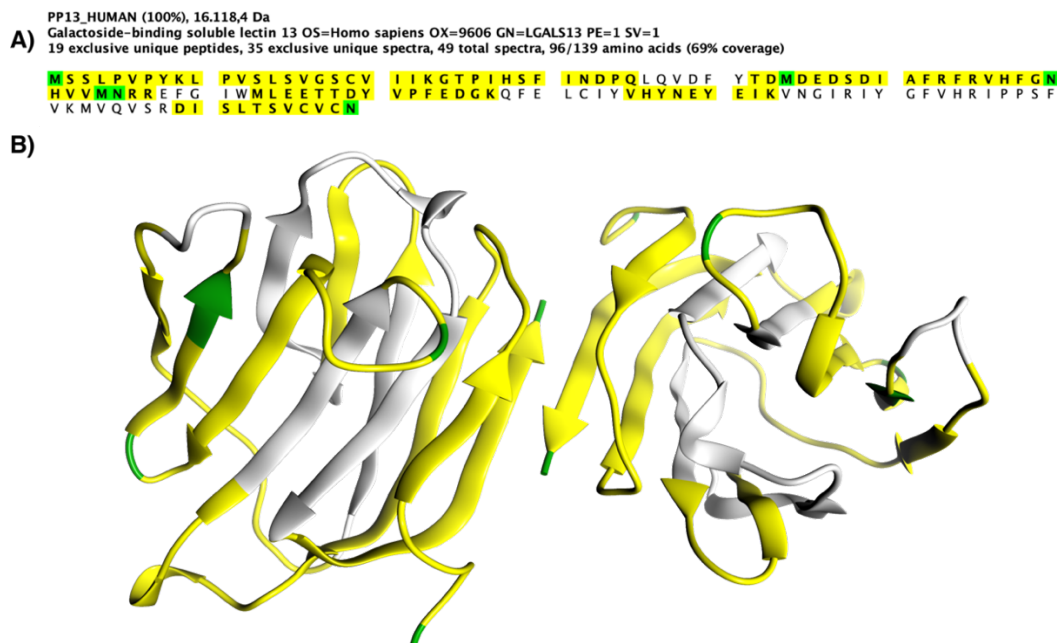
We concluded that purified recombinant protein had a molecular weight corresponding to GAL-13.

Figure 13. Mass spectrum of purified GAL-13.



We also performed a proteomics analysis of the purified protein to verify whether amino acid sequence corresponds to that of human galectin-13. Peptides identified through the analysis had 90-100 % identity with human PP13 (LGALS13 gene), with a 69 % coverage (96 of 139 amino acids) of the amino acid sequence, low coverage results from trypsin digestion of purified GAL-13, Figure 14 and Annex III. Our combined MS and proteomics analyses nevertheless confirm that the expressed protein is indeed human GAL-13.

Figure 14. Regions of purified GAL-13 that match with human galectin-13 protein sequence.



Sequenced regions are shown in yellow. Digestion of protein sample with trypsin produced 20 peptide fragments whose sequence identity to PP13 was 90 – 100 %. Sequenced peptides are colored in yellow, both on the amino acid sequence (A) and on the 3D structure (B), while regions in white correspond to the 43 residues of the protein that could not be sequenced.

2) GAL-13 characterization

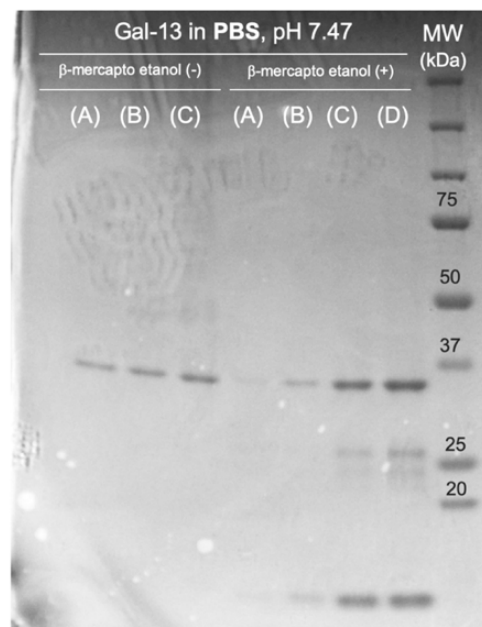
Once we confirmed that our GAL-13, was indeed human galectin-13 with proper sequence and molecular weight, we proceed to perform physicochemical characterization of our recombinant protein.

2.1) Evaluation of dimerization

We evaluated the dimerization state of purified protein using a semi-native SDS-PAGE. This was a necessary step since previous reports showed that GAL-13

monomers are inactive (Gizurason *et al.*, 2016; Drobnjak *et al.*, 2019) and reducing conditions used to purify GAL-13 might have influenced monomer-dimer equilibrium. We prepared dilution series with increasing concentrations of GAL-13, as an attempt to compare the effect of 2-mercaptoethanol and concentration, as dimerization equilibrium could be also affected by changes in protein concentration. Effect of concentration was not possible to assess due to small range in GAL-13 concentration. However, we confirmed that dimer populations are favored in absence of 2-mercapto ethanol, Figure 15.

Figure 15. Semi-native SDS-PAGE of GAL-13.

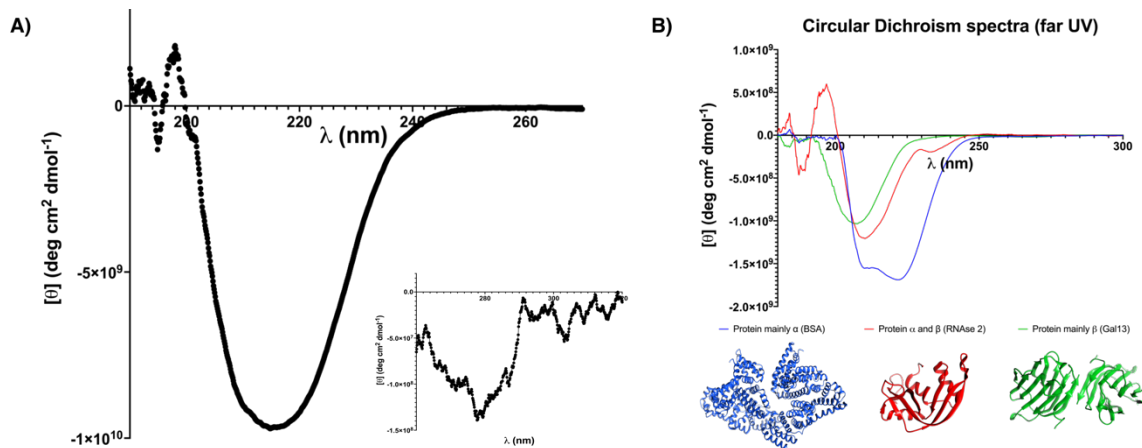


Samples with increasing concentrations of GAL-13: 2 μ M (A), 7 μ M (B), 12 μ M (C) and 24 μ M (D) were prepared in Laemmli buffer with or without 2-mercaptoethanol (indicated with +/- signs in labels).

2.2) Thermal stability of GAL-13

First, we evaluated secondary structure integrity of our recombinant GAL13 by collecting circular dichroism (CD) spectrum in the far UV region. Spectrum showed characteristic profile of a protein with a fold composed of antiparallel β -sheets (Figure 16-A), which consists of one peak with minimum between 210 and 225 nm. This is expected for galectin family as CRD fold consists of a β -sandwich. For the far UV spectrum of GAL-13, minimum was observed at $\lambda = 220$ nm, which is in same range as that observed in other family members, i.e. 216, 217 and 220 nm for galectins -1, -2 and -7, respectively (Di Lella *et al.*, 2010; Ermakova *et al.*, 2013; Sakakura *et al.*, 2018).

Figure 16. CD spectrum of GAL-13.

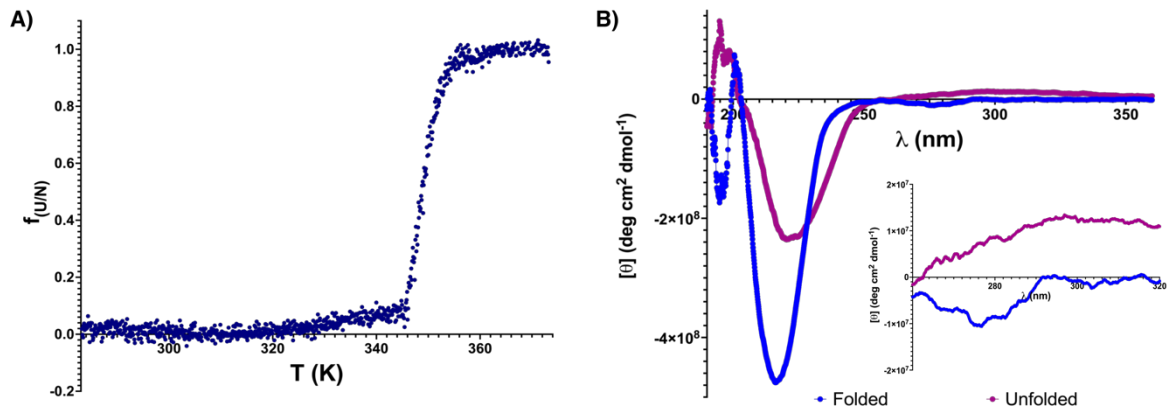


(A) The large plot shows far UV spectrum of recombinant GAL-13 in non-reducing conditions. Inset shows near UV spectrum of GAL-13 for the same sample. (B) Spectra of proteins with different secondary structures: motif mainly α -helix (bovine serum albumin) in blue, motif α -helices, and β -sheets (RNase 2) in red, and motif mainly β -sheets (GAL-13) in green.

A way to evaluate tertiary structure integrity consist of collecting near UV CD spectrum of recombinant protein (region $260 \leq \lambda \leq 320$ nm), it is also known as the fingerprint of a protein, due to the fact that signals in this region originate from vibrational states of aromatic residue side chains, which strongly rely on their number, spatial disposition in the protein, motility and their chemical environment (hydrogen bonding, polarizability of their neighbors). When some of these features change, it causes a change in the near UV signal profile. Phe shows sharp bands between 255 and 270 nm, Tyr residues show a peak between 275 and 282 nm, which could overlay with Trp fine peak at 290 – 305 nm (Kelly, Jess and Price, 2005). Near spectrum of our GAL-13 shows absorption in Phe and Tyr regions, but our characteristic Trp protein peak at 290 nm was not as intense and sharp as usually observed. This could be due to the fact that the Trp residue in GAL-13's GBS is already exposed to the solvent (Figure 16).

As part of our physicochemical characterization, a thermal unfolding experiment was carried out to provide hints on protein stability (Figure 17). We observed protein aggregation in samples incubated at 100 °C, an irreversible denaturation phenomenon that lasted when the temperature was cooled down to 20 °C (room temperature). After denaturation, our protein sample loss was estimated at 55.4 % of signal in far UV, with significant change in absorption profile of near UV spectrum. This is due to the change in the environment of GAL-13's aromatic residues upon denaturation (Li *et al.*, 2011). This could imply that at high temperature GAL-13 populations may exist as conformers which have lost tertiary structure, but retain significant secondary structure.

Figure 17. CD monitored thermal unfolding of GAL-13.



(A) Graph summarizes two independent experiments, performed in triplicate, where we evaluated changes in ratio of denatured and native GAL-13, $f_{(U/N)}$, upon increase of temperature. (B) Example of CD spectra of GAL-13 samples before (Folded) and after (Unfolded) thermal denaturation. Large plot shows far UV spectrum and small plot shows loss of GAL-13 fingerprint after denaturation (near UV spectrum).

Inflexion point of a denaturation curve represents the midpoint of transition, corresponding to the melting temperature (T_m) of protein thermal unfolding. The T_m value calculated for GAL-13 was $348.7 (\pm 0.1)$ K, which is in the same range as those of other galectin family members (Table 5). This value is the highest T_m relative to other prototypic galectins.

Table 5. Melting temperature values reported for galectins.

Galectin	T_m (K)	Reference
-13	$348.7 (\pm 0.1)$	Current study
-1	338	(Di Lella <i>et al.</i> , 2010)
-2 (mouse)	$339.85 (\pm 0.3)$	(Sakakura <i>et al.</i> , 2018)
-7	$342.45 (\pm 0.09)$	(Ermakova <i>et al.</i> , 2013)

We carried out another set of thermal unfolding assays of GAL-13 in presence of 1 mM 2-mercapto ethanol, in order to evaluate whether perturbation in monomer/dimer equilibrium affects overall thermal stability of GAL-13. Calculated

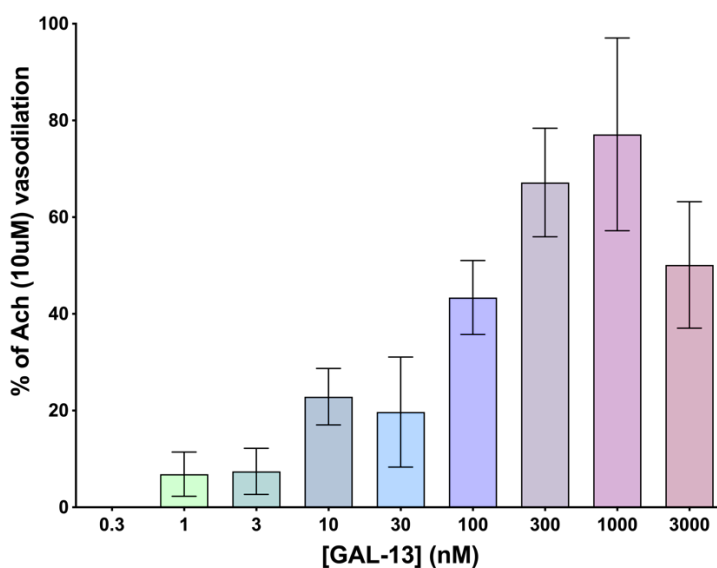
T_m was 347.3 (± 0.2) K, just 1 unit below from previous experiment, as we observed in non-reducing environment after thermal denaturation. This result suggests that the GAL-13 structure is unperturbed by these experimental conditions.

2.3) GAL-13 activity

Previously described set of MS, non-reducing electrophoresis, and CD experiments allowed us to assess structural integrity of our recombinant GAL-13. Next step for characterization consists to evaluate *in vitro* activity.

Through a set of dilation assays (Figure 18), we confirmed that GAL-13 under non-reducing conditions induced a concentration dependent vasodilation effect on rat aortas, which supports previously reported induction of mesenteric arteries dilation (Drobnjak *et al.*, 2017).

Figure 18. Rat aorta vasodilation assay.



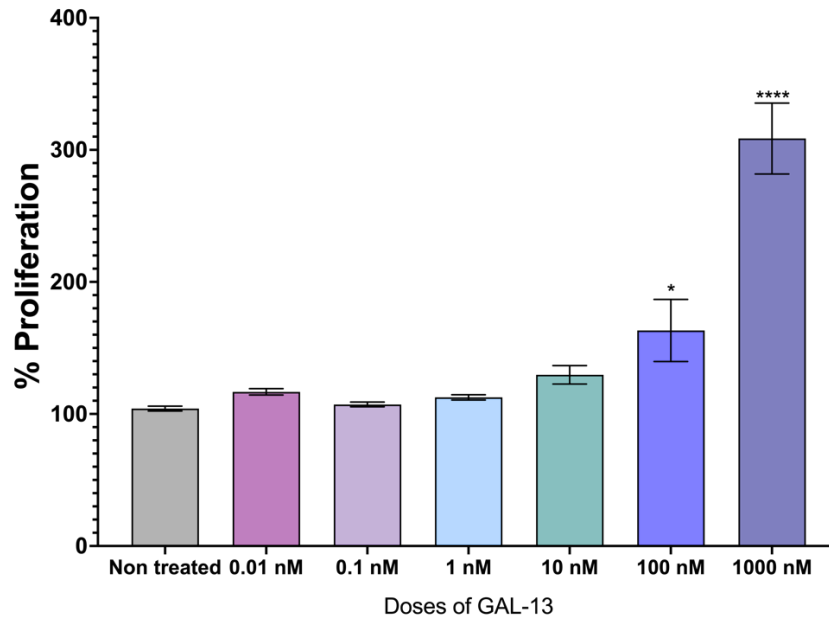
Results from five independent experiments of isolated aortas from Sprague-Dawley rats (7-8 weeks old) treated with increasing concentrations of GAL-13. Vasodilation is expressed as the percentage of the response induced by 10 μ M acetylcholine on the KCl (30 mM) contracted aorta ring.

By using thoracic aortas from male rats, we observed similar profiles as (Drobnjak *et al.*, 2017). However, we used GAL-13 doses approximately 10-fold higher to achieve the same dilation effect. This outcome make sense since, by controlling blood flow to different organs, the mesenteric arteries are more susceptible to dilation and contraction, while the aorta mainly supplies blood to other blood vessels and, only in extreme cases, relaxes or contracts to compensate for changes in blood pressure.

It has been reported that GAL-13 plays a role in placentation. Placentation or placental development is the process through which the embryo survives by attaching to the uterus and reaches maternal circulation to promote nutrient, waste and gas exchange. This occurs thanks to trophoblast cells (direct precursors of placenta), which proliferate and differentiate to invade endometrium, where they are capable of “searching” for vessels (McMaster and Fisher, 2003; Frank, 2017). As a result, another way to verify activity of GAL-13 consists in evaluating trophoblast cells proliferation, migration and/or invasiveness.

We evaluated GAL-13 effect on cell line derived from human placental choriocarcinoma (JEG-3) under non reducing conditions, as a cell model of the invasive and proliferative extra villous trophoblast. GAL-13 increase populations of living JEG-3 cells in a concentration dependent manner, reaching significant effect at 100 and 1000 nM (Figure 19), suggesting a role of GAL-13 in placentation.

Figure 19. Increase of JEG-3 cells proliferation by GAL-13.



Relative JEG-3 cell proliferation rates are expressed as mean \pm SEM (n= 6). Asterisks (*, ****) statistically significant difference between treated cells and negative control calculated by one-way ANOVA (*P < 0.05, **P < 0.01), n=5 independent experiments.

The assay was performed in absence of serum for three days and live cells were detected by using resazurin reagent. The effect of GAL-13 was as high as 3 folds comparing with non-treated control, meaning that after 72h number of living cells its higher in presence of GAL-13. Additional probes are needed, such as a time course analysis, in order to better understand the mechanism of this protein over JEG-3 cells, and to elucidate whether GAL-13 indeed increased cell proliferation or if it rather protected cells from dying.

Further assays with trophoblasts cells i.e. cell migration and invasion will provide additional interesting lights to understand GAL-13 (PP13) role in placentation.

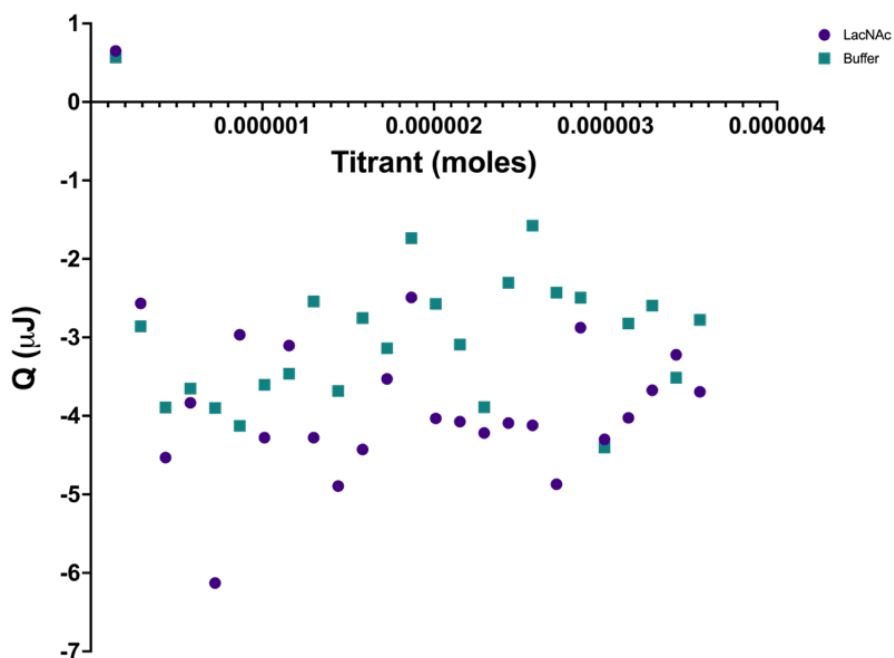
However, along with vasodilation assay, this preliminary set of results allow us to assess activity of our recombinant galectin-13.

3) Binding Assays

Galectins are characterized by their affinity towards β -galactosides (Vasta *et al.*, 2012). Even though most galectin family members typically exhibit micromolar affinities towards α -lactose and other β -galactosides, GAL-13 showed no binding to this sugar. Indeed, double and triple mutants were constructed to promote GAL-13 co-crystallization with lactose (Su, Cui, *et al.*, 2018).

Previously, Than and coworkers concluded that GAL-13 prefers binding aminated glycans than regular carbohydrates (Than *et al.*, 2004). They reported that GAL-13 exhibits decreasing affinity order towards N-acetyl lactosamine (LacNAc), D-mannose, N-acetyl galactosamine (GalNAc), D-maltose, D-glucose, D-galactose, D-fucose and α -D-lactose, but dissociation constants (K_D) were not determined. Also, the mode of carbohydrate binding to GAL-13 has yet to be described. Therefore, we moved to characterize binding affinity in an attempt to assess determination of K_D values to GAL-13. We first evaluated LacNAc binding since GAL-13 apparently has the highest affinity towards this disaccharide (Than *et al.*, 2004).

Figure 20. Isothermal titration of GAL-13 with LacNAc.



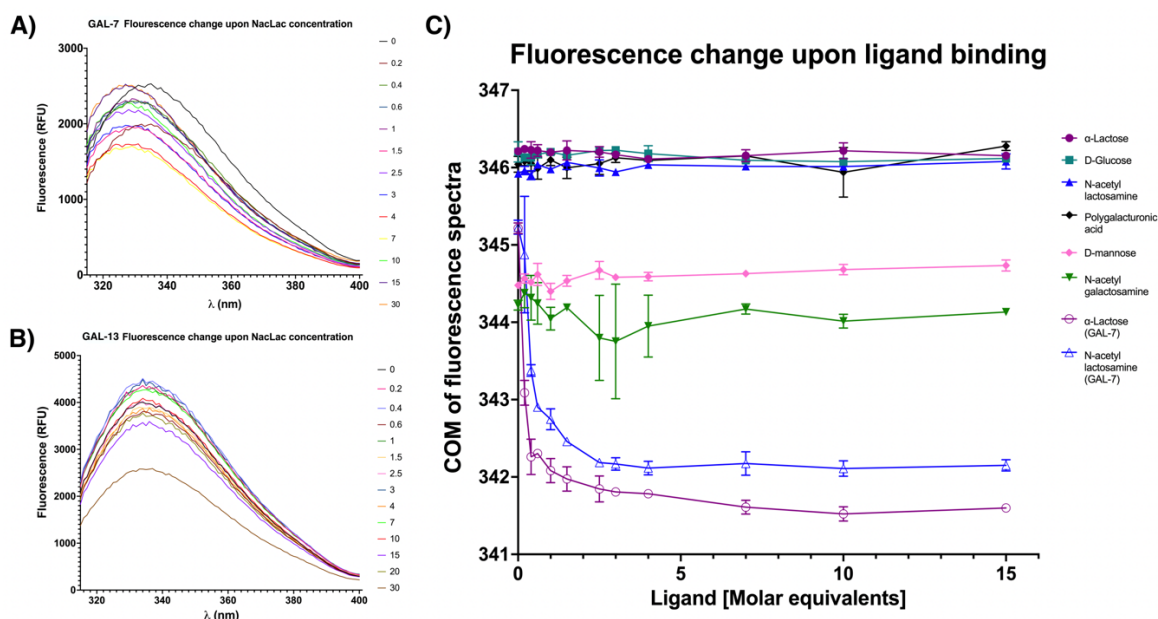
Circles in purple show data of GAL-13 titration with LacNAc, jade green squares correspond to data of GAL-13 titration with buffer.

We performed several unsuccessful ITC (Figure 20) and MST assays (Annex IV), leading us to conclude that LacNAc does not bind to GAL-13. To assess binding between PP13 (GAL-13) and different glycans, Than *et al.* used a chromatographic approach. This procedure might lead to false positives, as it consisted in the determination of relative binding rates as function of fluorescence signal change upon centrifugation of samples vigorously shaken for 1h in presence of sugar-modified agarose beads (Than *et al.*, 2004).

Our results, inconsistent with Than and co-workers, prompted us to standardize a fluorescence assay to qualitatively assess screening of GAL-13 binding to a larger catalogue of sugars. This effectively provided us with a cheap and low sample consuming approach, and thus contrasting results with aforementioned report.

The main basis to determine GAL-13 binding by fluorescence consists in detection of tryptophan (W) fluorescence emission quenching due to ligand binding. Galectin family members share a consensus tryptophan residue in GBS, which is relevant to promote ligand binding via π - π stacking between electron density within indole ring of W and hemiacetal ring of sugar moieties in ligand. Since intrinsic fluorescence of proteins is mainly due to aromatic residues (Y, F and W), we selectively traced W quenching by using an excitation wavelength of 295 nm, instead of regular 280 nm, which could overlap with Y absorption.

Figure 21. Fluorescence binding assay.



(A) Quenching shift of GAL-7 (used as positive control) upon binding to LacNAc, maximum wavelength of emission shifts from 342 to 323 nm when ligand binds. (B) Fluorescence spectra of GAL13 titration with LacNAc, maximum wavelength of emission did not shift from 338 nm. (C) Center of mass (COM) of fluorescence spectra. GAL-13 titrated with any carbohydrates (filled shapes) tested did not show change in fluorescence. GAL-7 was used as positive control.

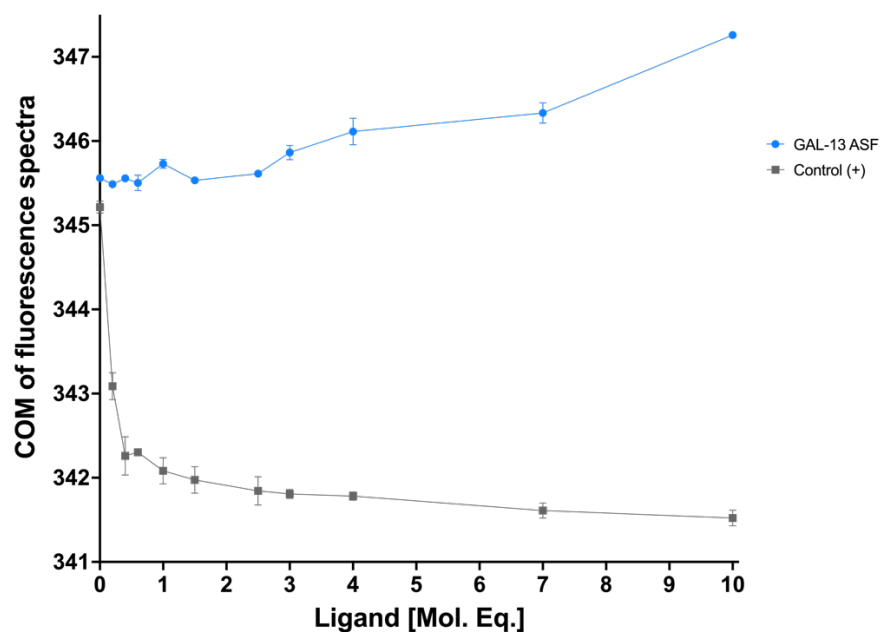
We used GAL-7 both as standard for experimental set-up and as a positive control. This allowed us to determine detection limit (20 μ M of recombinant prototype galectin), as well as to observe that the maximum wavelength of fluorescence spectrum shifts down approximately 15 nm, from 342 to 323 nm, in the case of LacNAc binding (Figure 21-A). This small shift is consistent with quenching changes observed upon ligand binding to GAL-2, -3 and -4 (Sindrewicz *et al.*, 2019).

In contrast to the previously cited report (Than *et al.*, 2004), absence of quenching in spectra and COM change upon GAL-13 titration confirmed that our protein did not show binding towards the following carbohydrates: α -D-lactose, N-acetyl lactosamine, D-glucose, D-mannose, N-acetyl galactosamine and polygalacturonic acid (Figure 21). These findings are consistent with the fact that placenta is a tissue rich in moieties of sialic acid linked $\alpha(2,6)$ to N-acetyl-D-galactosamine, N-acetyl-D-glucosamine and D-galactose (Sgambati *et al.*, 2007; Marini *et al.*, 2011).

Regardless, since the GBS of GAL-13 shows high amino acid and structural identity relative to other galectins, one should expect this strong conservation to act as a determinant in GAL-13 function. As a result, evaluating the functional role of conserved residues in the GAL-13 GBS is of significant importance. Although we have not been able to reproduce *in vitro* binding of small galactoside sugars to GAL-13, proper binding to complex sugar moieties might still be required for proper cellular function of this protein. A common ligand among galectins is asialofetuin (ASF), also known as fetuin-A or 2 α -HS-Glycoprotein (AHSG), a 46 kDa protein playing multiple physiological roles (Jirak *et al.*, 2019). ASF is a protein with nine glycosylated sites, at three Asn, four Ser and two Thr residues.

Glycan motifs of ASF contain N-acetyl glucosamine, mannose and galactose units in high proportion. Galectin binding towards ASF is explained as a result of high family member affinity towards carbohydrates. Thus, we moved to evaluate GAL-13 binding towards ASF.

Figure 22. Fluorescence binding assay of GAL13 with ASF.



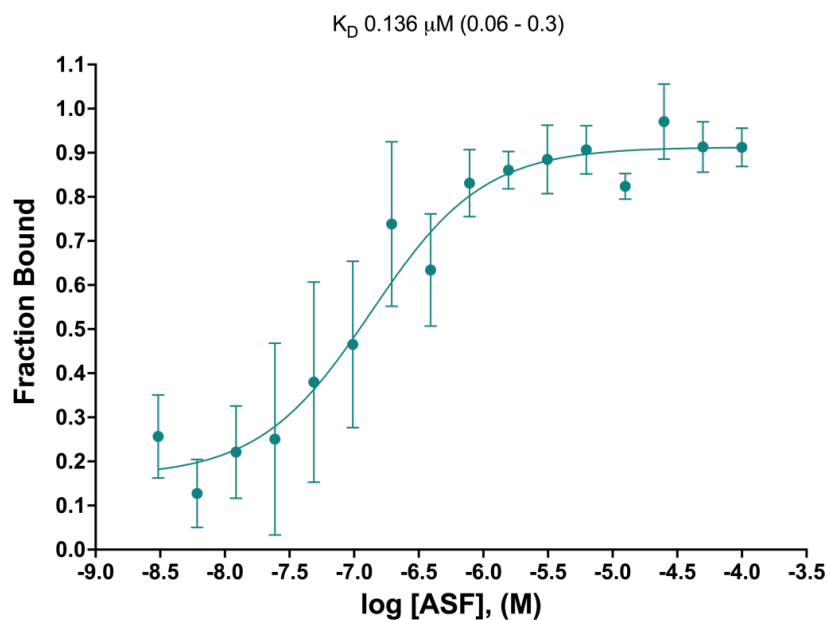
Fluorescence monitored titration of GAL-13 with ASF. Plot shows change in COM of spectra from each titration point. Positive control corresponds to GAL-7 titration with α -D-lactose.

A preliminary ELISA assay allowed us to observe positive binding between our protein and ASF. In parallel, we also performed a fluorescence monitored titration of GAL-13 with ASF (Figure 22). We found that fluorescence COM increased upon ASF concentration, which is opposite to previously observed patterns. ASF is a protein with two Trp residues at positions 14 and 69, suggesting that their hydrophobic environment changes upon binding to GAL-13.

To further characterize ASF binding to GAL-13, we first carried out an ITC experiment. We observed a change in cell heat upon increase of ASF concentration (approximately 40 μJ difference, Annex V). However, we could not set up experiment conditions due to ASF precipitation at high concentrations.

Therefore, we carried out microscale thermophoresis (MST) experiments to assess binding affinity. MST requires much lower protein concentrations than ITC, effectively overcoming the protein precipitation issues we observed with the latter technique. Consequently, we successfully calculated a $K_D = 0.136 \mu\text{M}$ for the binding between GAL-13 and ASF (Figure 23). We concluded that GAL-13 has the strongest affinity towards ASF among all reported prototype galectins, since our value is the lowest reported K_D among all family members (Table 6).

Figure 23. Dose response curve from MST data.



Graph summarizes five independent binding tests performed by triplicate under the same conditions (buffer, temperature and fixed concentrations of GAL-13 and ASF solutions).

Through binding assays we found out that our recombinant galectin-13 recognizes N-glycans attached to asialofetuin but not to free mono- and disaccharides, this is consistent with the fact that glycosylated proteins contains patterns with more than three carbohydrates bounded.

Table 6. Dissociation constants reported for human galectins (Dam *et al.*, 2005).

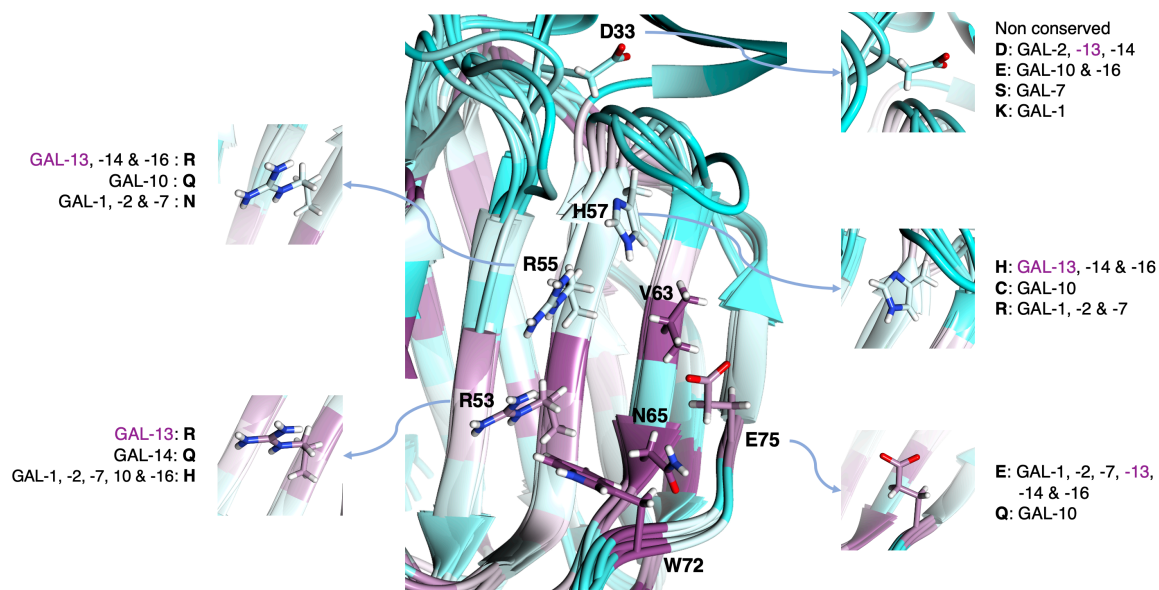
Galectin	K _D (μM)	
	ASF	LacNAc
-1	1.786	100
-2	0.714	52.632
-3	0.714	55.556
-4	4.545	285.714
-7	3.333	238.095
-13 (this study)	0.136	N/A

4) Mutants

In order to evaluate whether conserved residues in the GBS are necessary for GAL-13 function, we moved to design loss-of-function alanine single point mutants. Among galectin family, six positions are involved in glycan binding, five of which promote binding through formation of hydrogen bonding and one consensus aromatic residue that stabilizes binding through hydrophobic interactions.

Differences between residues in the GAL-13 GBS and those from other prototype galectins are highlighted in Figure 24. Some key positions that form hydrogen bonding interactions with the glycan ligand are different in GAL-13, such as R53, R55 and H57, positions that correspond to His, Asn and Arg residues respectively in galectins -1, -2 and -7 sequences.

Figure 24. Close up to GAL-13's GBS from overlay of human prototypic galectins.



Showing side chain of residues involved in ligand binding (labels correspond to numbering of GAL-13 sequence). Superimposed structures were: GAL-1 (1GZW), GAL-2 (5DG1), GAL-7 (4GAL), GAL-10 (1LCL), GAL-13 (5XG7), GAL-14 (6K2Y) and GAL-16 (6LJP).

We considered both relevance in ligand recognition/binding and conservation of each residue among family to choose positions for construction of GBS mutants. Residues targeted were R53, R55, H57, V63, N65 and E75. N65 and E75 are conserved positions which directly interact with ligand. In other family members, residue 53 is conserved as a His, forming a hydrogen bond with ligand, but in GAL-13 this position is an Arg. Valine at position 63 in GAL-13 is a consensus residue that does not interact directly with ligand. Finally, we selected GAL-13 residues at

positions 55 and 57 as mutational targets because they are involved in direct hydrogen bonding interactions with glycans in galectins -1, -2 and -7.

4.1) Over-expression and purification of GBS mutants

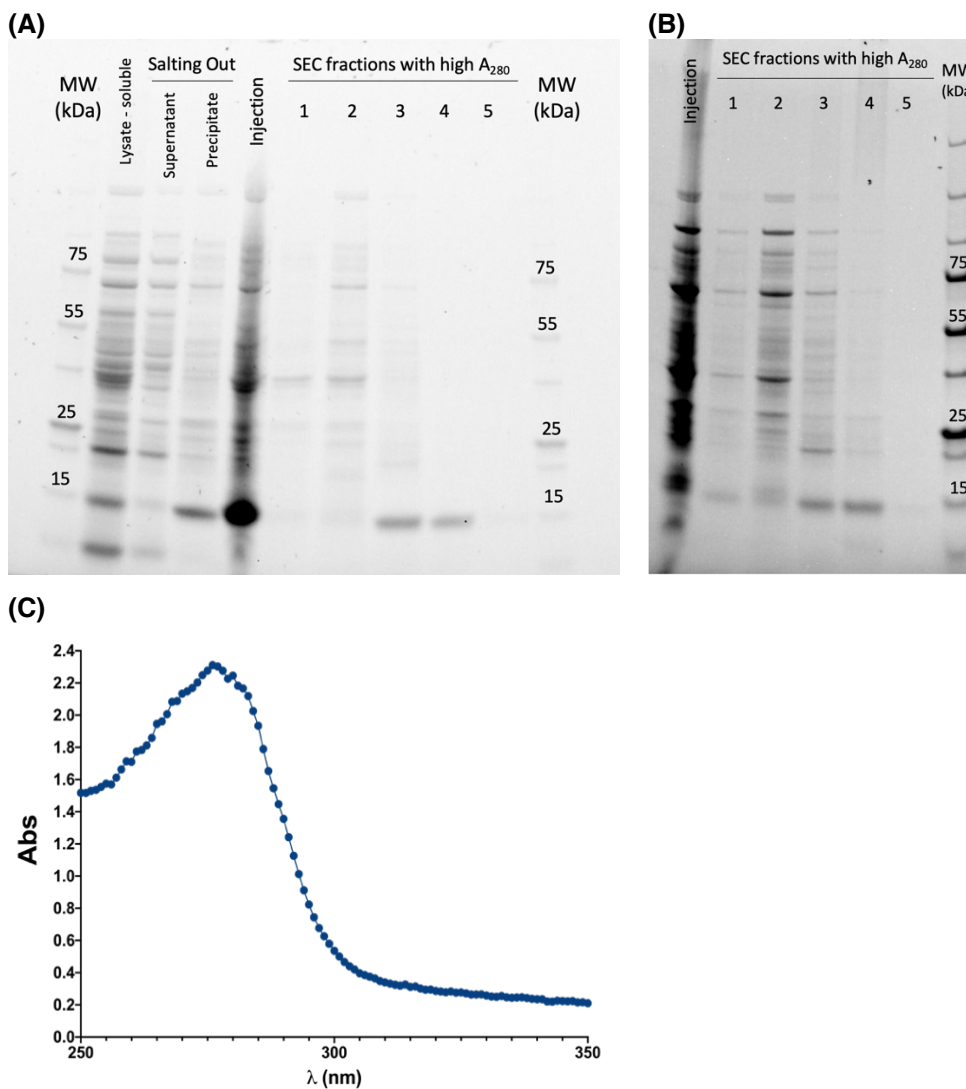
We did not obtain GAL-13 mutants R53A, H57A and E75A by following NEB Q5® site directed mutagenesis kit. Through DNA sequencing, we verified the presence of single point mutations in DNA isolated from positive clones obtained from site-directed mutagenesis, which confirmed that we successfully cloned R55A, V63A and N65A variants of GAL-13. Then we proceeded to assess over-expression conditions of mutants by evaluating their induction and expression profiles.

Three different *E. coli* strains, BL21 (DE3), Origami 2 (DE3) and Rosetta-gami (DE3) were used to evaluate mutant over-expression under two different conditions: incubation at 16 °C and 37 °C, and monitoring induction at 4 h and 16 h after IPTG addition, from which we concluded that the best conditions to over-express mutants consisted in the use of *E. coli*/BL21 (DE3) system and 16 h induction of recombinant protein expression by addition of IPTG to a final concentration of 0.2 mM. There was no significant change between cultures induced at 16 °C or 37 °C.

To purify R55A, V63A and N65A variants, we moved to apply the same protocol as for wt-GAL-13 (Figure 25). We first remarked that all mutants were more susceptible to precipitate during the purification process than wt-GAL-13, especially R55A. Purification conditions of mutants R55A and N65A still require optimization.

Protocol for wild-type purification worked well for purification of mutant V63A without any modification. We expressed similar yields as wt-GAL-13, i.e. from 2.5g of cell pellet, we obtained 15 to 30 mL of pure protein at 2.7 mg mL⁻¹ (Figure 25-A and C). For mutant N65A, we managed to improve enrichment of recombinant protein by increasing the percentage of saturation with ammonium sulfate during the salting out step, but purification conditions still need optimization (Figure 25-B).

Figure 25. Purification of GAL-13 mutants.

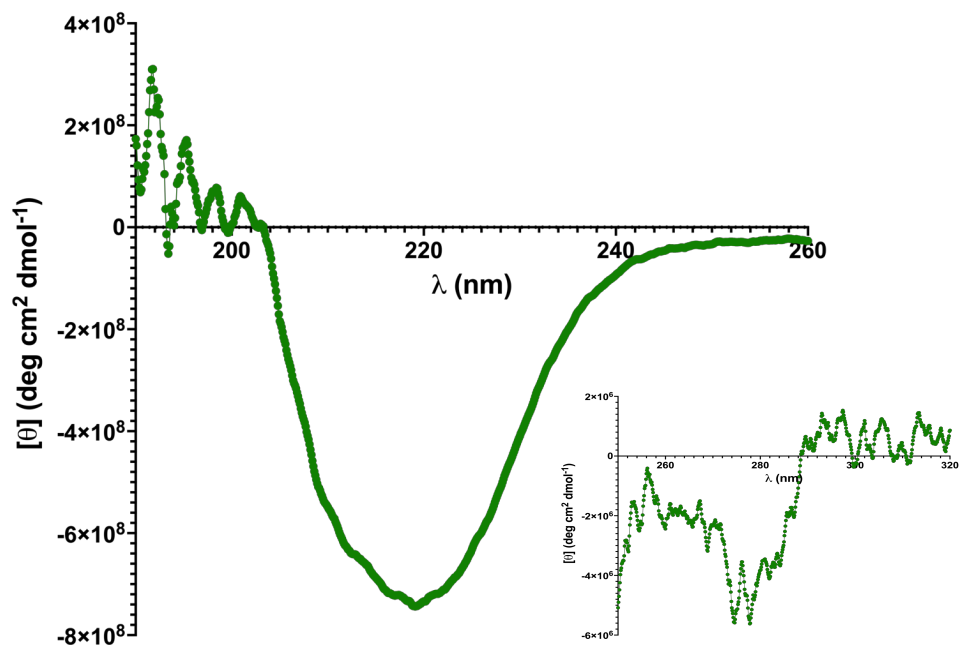


SDS-PAGE verification of: (A) Purification of variant V63A; (B) Size exclusion purification of variant N65A. (C) UV spectrum collected for quantification of mutant V63A.

4.2) Preliminary characterization

To assess secondary structure integrity of GAL-13-V63A, we collected CD spectra. Far UV CD spectrum correspond to the wt-GAL-13 absorption profile, which is characteristic of a protein with a mainly β -strand fold, i.e. one minimum at 220 nm, as observed in wt-GAL-13 spectrum. Near UV spectrum was collected to evaluate tertiary structure integrity (Figure 26). For GAL-13-V63A, near UV spectrum shows a signal corresponding to Phe and Tyr residues in a similar fashion as observed for wild type, suggesting that mutant V63A maintains secondary and tertiary structure after purification.

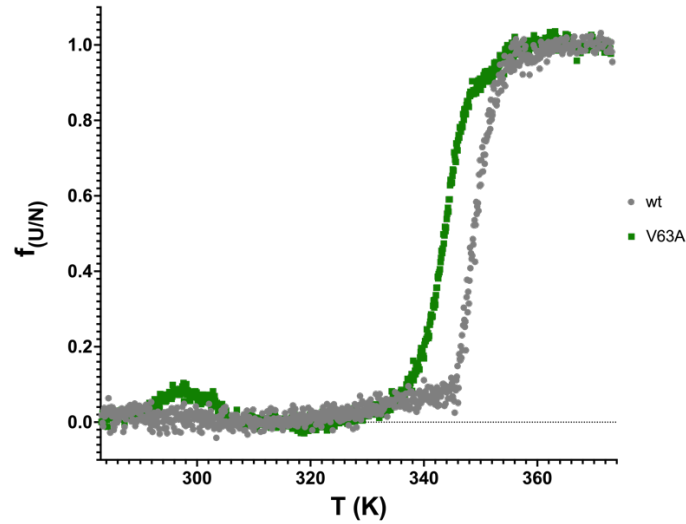
Figure 26. CD spectrum of GAL-13-V63A.



Large plot shows far UV spectrum and small graph shows near UV spectrum of corresponding mutant.

To investigate whether overall thermal stability was modified upon mutation, we performed thermal denaturation of GAL-13-V63A (Figure 27). Increase in temperature induces an irreversible denaturation of this protein, as observed with wt-GAL-13. After denaturation, V63A aggregates have lost tertiary structure but conserved significant secondary structure elements. Data collected from this experiment allowed us to calculate a T_m value of $343.6 (\pm 0.1)$ K for this mutant, which is five degrees lower than wild type.

Figure 27. Thermal unfolding of GAL13-V63A monitored by CD.

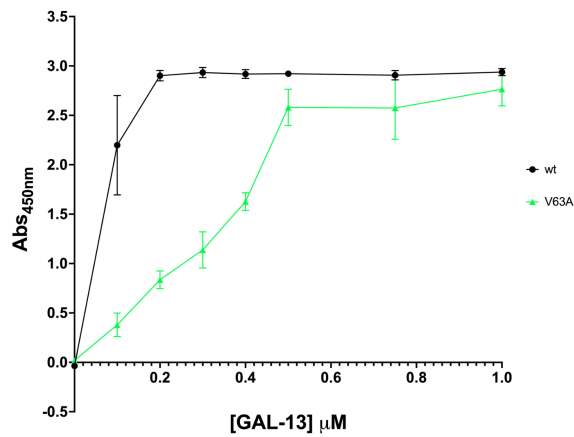


Data of mutant corresponds to a single experiment performed in triplicate.

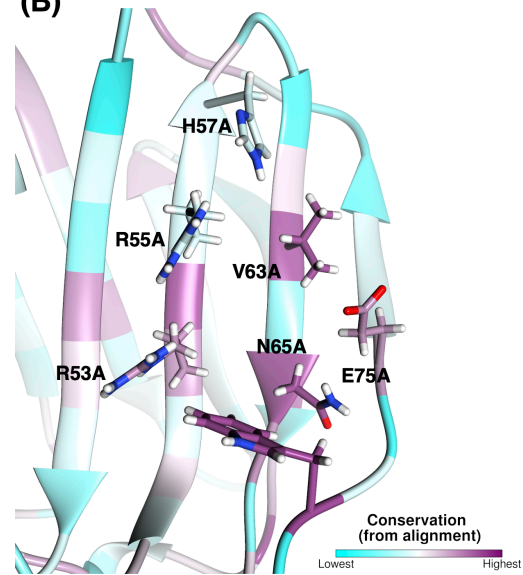
When we evaluated binding of wt-GAL-13, we found out that fluorescence assay does not allow us to qualitatively assess binding of ASF to GAL-13 due to the presence of two Trp residues on the ASF sequence, which we do not know whether they change their environment upon binding or not. Therefore, we performed an ELISA test to evaluate binding of V63A towards ASF (Figure 28).

Figure 28. GAL-13-V63A binding towards ASF.

(A) ELISA wt- and GAL-13-V63A



(B)



Evaluation of mutants binding towards ASF (A), and positions chosen in the GBS of GAL-13 to construct point mutations (B).

Although GAL-13-V63A is capable of binding to ASF, affinity decreased relative to wild type. This result confirms that V63^{hGAL-13} is involved in binding, even though it was shown not to be directly involved in ligand recognition in other galectin family members. Results from this experiment allow to hypothesize that ligand positioning in GAL-13 may differ from other galectins.

However, further structural and functional analysis are still required to accurately characterize ASF binding to GAL-13. Optimization of purification protocols for mutants are also still to be done before moving to determination of K_D values.

CONCLUSIONS AND PERSPECTIVES

In this project, we over-expressed and purified non-tagged recombinant GAL-13 and set up experimental conditions to evaluate ASF binding, aorta vasodilation, and trophoblast cell proliferation. This will allow further evaluation of functional role of conserved residues within its glycan binding site (GBS). Additional assays with trophoblasts cells i.e. cell migration and invasion will provide additional interesting data to understand GAL-13 (PP13) role in placentation.

We determined a dissociation constant value of 0.136 μM between wt-GAL-13 and ASF. Further structural analysis of GAL-13-ASF complex through crystallographic studies could provide interesting and valuable data to understand evolutionary divergence in the GAL-13 GBS.

To evaluate the role played by glycan binding in the biological function of GAL-13, it could be interesting to perform activity assays in the presence of ASF. In correlation with structural data, this would provide insights on the role of conserved GBS residues in GAL-13 function.

Three of six designed mutants were already expressed. Mutant V63A was purified but activity assays are still to be undertaken. Optimization of purification conditions for mutants R55A and N65A are also still needed.

ANNEXES

Annex I

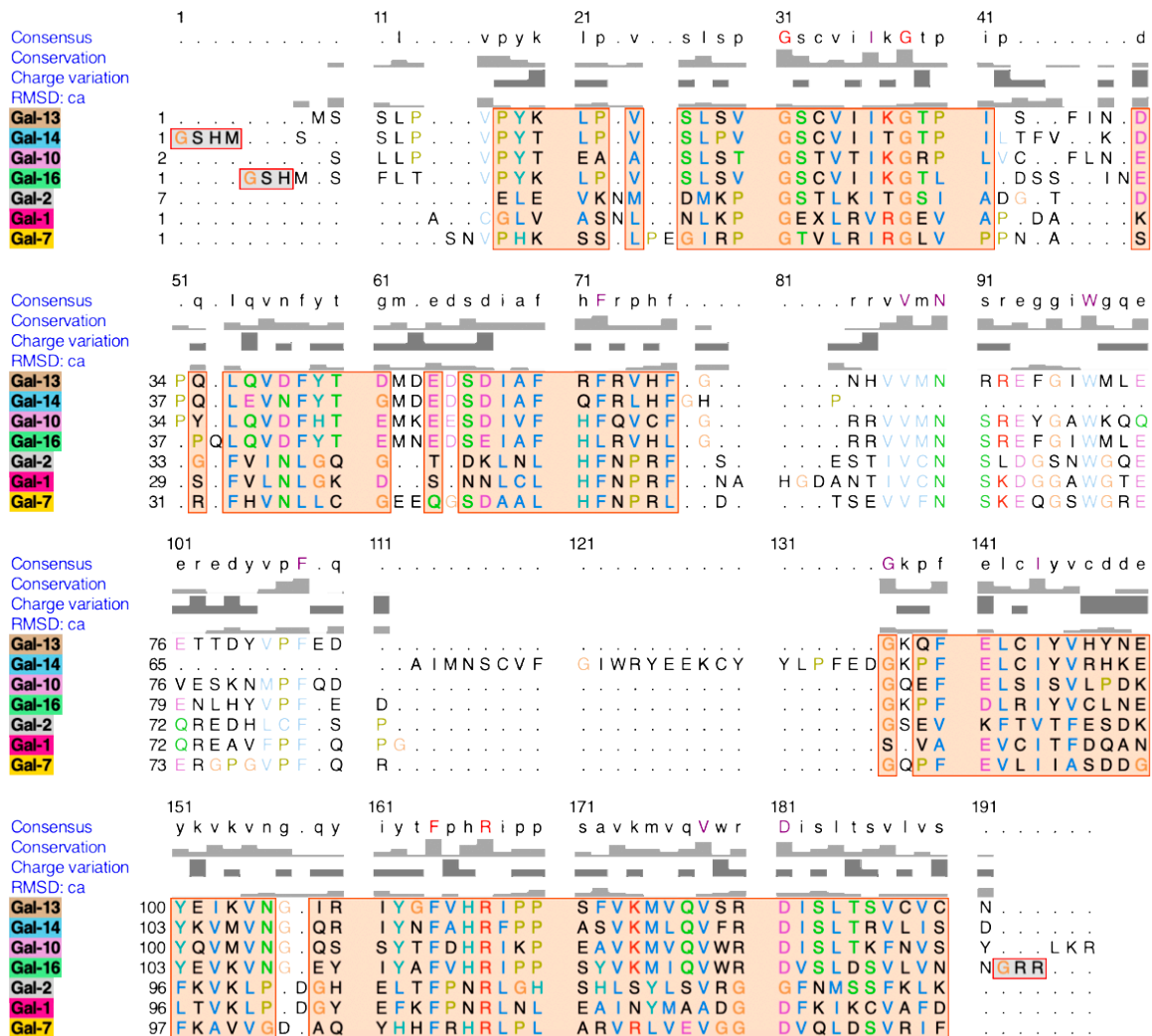


Figure 29. Sequence alignment from an overlay of galectin structures.

Alignment of galectins -1 (1GZW), -2 (5DG1), -7 (4GAL), -10 (1LCL), -13 (5XG7), -14 (6K2Y) and -16 (6LJP) structurally superimposed was performed with UCSF Chimera (Pettersen et al., 2004). Capital letters were used to show consensus and highly conserved residues. Light orange colored boxes show regions with low RMSD values.

Annex II

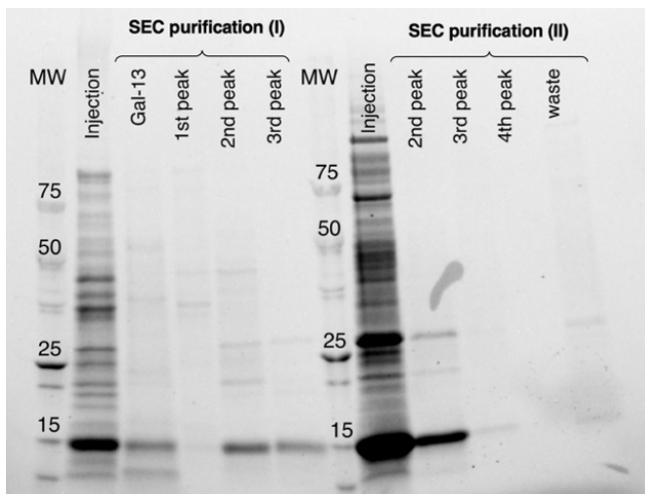


Figure 30. GAL-13 SEC purifications to assess method reproducibility.

Annex III

Index	Peptide	Exclusive To	Valid	Galac... No Gr...
9	IYGFVHR	Galactoside-binding soluble lectin 13 ...	✓	90%
8	GTPIHSFINDPQ	Galactoside-binding soluble lectin 13 ...	✓	97%
2	DISLTSVCV	Galactoside-binding soluble lectin 13 ...	✓	98%
7	GNHVVMNR	Galactoside-binding soluble lectin 13 ...	✓	99%
14	SSLPVYPYKLPVSLVSGSCVIK	Galactoside-binding soluble lectin 13 ...	✓	99%
1	DESDIAFR	Galactoside-binding soluble lectin 13 ...	✓	100%
3	DISLTSVCVC	Galactoside-binding soluble lectin 13 ...	✓	100%
4	DISLTSVCVCN	Galactoside-binding soluble lectin 13 ...	✓	100%
5	DMDESDIAFR	Galactoside-binding soluble lectin 13 ...	✓	100%
6	FRVHFGNHVVMNR	Galactoside-binding soluble lectin 13 ...	✓	100%
10	LPVSLVSGSCVIK	Galactoside-binding soluble lectin 13 ...	✓	100% (100%)
11	MDESDIAFR	Galactoside-binding soluble lectin 13 ...	✓	100%
12	MLEETTDYVPFEDGK	Galactoside-binding soluble lectin 13 ...	✓	100%
13	MSSLPVYPYK	Galactoside-binding soluble lectin 13 ...	✓	100%
15	TDMDESDIAFR	Galactoside-binding soluble lectin 13 ...	✓	100%
16	VHFGNHVVM	Galactoside-binding soluble lectin 13 ...	✓	100%
17	VHFGNHVVMN	Galactoside-binding soluble lectin 13 ...	✓	100%
18	VHFGNHVVMNR	Galactoside-binding soluble lectin 13 ...	✓	100%
19	VHFGNHVVMNRR	Galactoside-binding soluble lectin 13 ...	✓	100%
20	VHYNEYEIK	Galactoside-binding soluble lectin 13 ...	✓	100%

Figure 31. MS/MS sequenced fragments from GAL-13 digestion with trypsin.

Annex IV

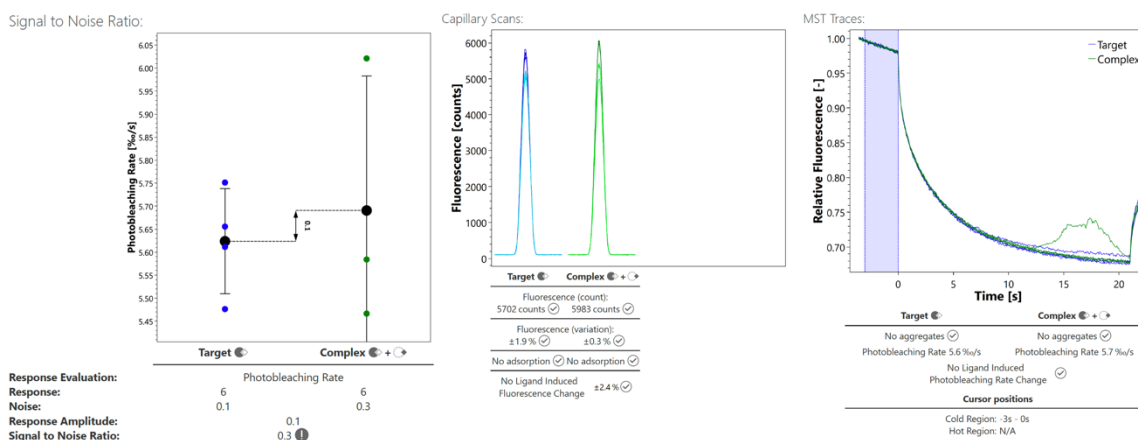


Figure 32. MST binding check of LacNAc to GAL-13.

Annex V.

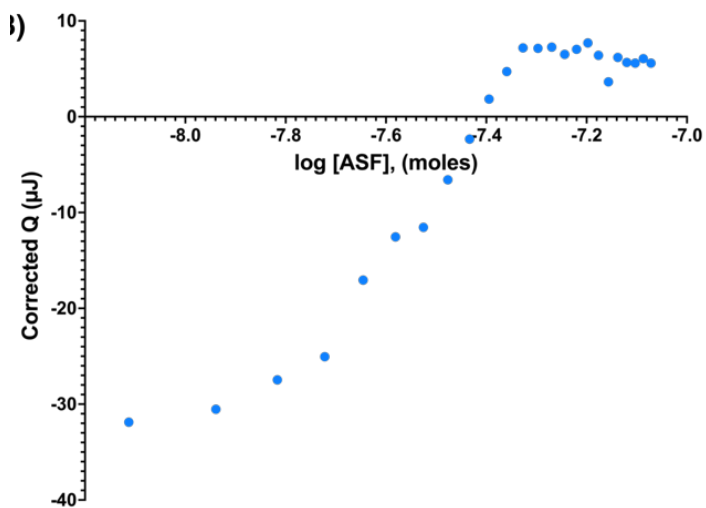


Figure 33. ITC experiment to characterize GAL-13 binding to ASF.

Results show a change in cell heat capacity upon increase of ASF concentration.

REFERENCES

- Arthur, C. M. et al. (2015) "Evolving mechanistic insights into galectin functions," *Methods Mol Biol.* 2014/09/26, 1207, pp. 1–35. doi: 10.1007/978-1-4939-1396-1_1.
- Balogh, A. et al. (2011) "Placental protein 13 (PP13/galectin-13) undergoes lipid raft-associated subcellular redistribution in the syncytiotrophoblast in preterm preeclampsia and HELLP syndrome," *Am J Obstet Gynecol.* 2011/05/21, 205(2), pp. 156 e1–14. doi: 10.1016/j.ajog.2011.03.023.
- Balogh, A. et al. (2019) "Placental Galectins Are Key Players in Regulating the Maternal Adaptive Immune Response," *Front Immunol.* 2019/07/06, 10, p. 1240. doi: 10.3389/fimmu.2019.01240.
- Bartolazzi, A. (2018) "Galectins in Cancer and Translational Medicine: From Bench to Bedside," *Int J Mol Sci.* 2018/09/29, 19(10). doi: 10.3390/ijms19102934.
- Blois, S. M. et al. (2019) "Pregnancy Galectinology: Insights Into a Complex Network of Glycan Binding Proteins," *Front Immunol.* 2019/06/25, 10, p. 1166. doi: 10.3389/fimmu.2019.01166.
- Bohn, H., Kraus, W. and Winckler, W. (1983) "Purification and characterization of two new soluble placental tissue proteins (PP13 and PP17)," *Oncodev Biol Med.* 1983/01/01, 4(5), pp. 343–350. Available at: <https://www.ncbi.nlm.nih.gov/pubmed/6856484>.
- Burger, O. et al. (2004) "Placental protein 13 (PP-13): effects on cultured trophoblasts, and its detection in human body fluids in normal and pathological pregnancies," *Placenta.* 2004/06/15, 25(7), pp. 608–622. doi: 10.1016/j.placenta.2003.12.009.
- Chan, Y. C. et al. (2018) "Dissecting the Structure-Activity Relationship of Galectin-Ligand Interactions," *Int J Mol Sci.* 2018/02/01, 19(2). doi: 10.3390/ijms19020392.
- Chetry, M. et al. (2018) "The Role of Galectins in Tumor Progression, Treatment and Prognosis of Gynecological Cancers," *J Cancer.* 2018/12/28, 9(24), pp. 4742–4755. doi: 10.7150/jca.23628.
- Dam, T. K. et al. (2005) "Galectins bind to the multivalent glycoprotein asialofetuin with enhanced affinities and a gradient of decreasing binding constants," *Biochemistry.*

- 2005/09/15, 44(37), pp. 12564–12571. doi: 10.1021/bi051144z.
- Drobnjak, T. et al. (2017) “Placental protein 13 (PP13)-induced vasodilation of resistance arteries from pregnant and nonpregnant rats occurs via endothelial-signaling pathways,” *Hypertens Pregnancy*. 2017/05/20, 36(2), pp. 186–195. doi: 10.1080/10641955.2017.1295052.
- Drobnjak, T. et al. (2019) “Placental protein 13 (PP13) stimulates rat uterine vessels after slow subcutaneous administration,” *Int J Womens Health*. 2019/04/17, 11, pp. 213–222. doi: 10.2147/IJWH.S188303.
- Ermakova, E. et al. (2013) “Lactose binding to human galectin-7 (p53-induced gene 1) induces long-range effects through the protein resulting in increased dimer stability and evidence for positive cooperativity,” *Glycobiology*. 2013/02/05, 23(5), pp. 508–523. doi: 10.1093/glycob/cwt005.
- Fischer, I. et al. (2010) “Stimulation of syncytium formation in vitro in human trophoblast cells by galectin-1.,” *Placenta*, 31(9), pp. 825–832. doi: 10.1016/j.placenta.2010.06.016.
- Flores-Ibarra, A. et al. (2018) “Crystallization of a human galectin-3 variant with two ordered segments in the shortened N-terminal tail,” *Sci Rep*. 2018/07/01, 8(1), p. 9835. doi: 10.1038/s41598-018-28235-x.
- Frank, H.-G. (2017) “10 - Placental Development,” in Polin, R. A. et al. (eds.). Elsevier, pp. 101–113. doi: <https://doi.org/10.1016/B978-0-323-35214-7.00010-X>.
- Gasteiger, E. et al. (2005) “Protein Identification and Analysis Tools on the ExPASy Server,” in Walker, J. M. (ed.) *The Proteomics Protocols Handbook*. Totowa, NJ: Humana Press, pp. 571–607. doi: 10.1385/1-59259-890-0:571.
- Gebhardt, S., Bruiners, N. and Hillermann, R. (2009) “A novel exonic variant (221delT) in the LGALS13 gene encoding placental protein 13 (PP13) is associated with preterm labour in a low risk population,” *J Reprod Immunol*. 2009/10/13, 82(2), pp. 166–173. doi: 10.1016/j.jri.2009.07.004.
- Gizurarson, S. et al. (2016) “Placental Protein 13 Administration to Pregnant Rats Lowers Blood Pressure and Augments Fetal Growth and Venous Remodeling,” *Fetal Diagn Ther*. 2015/09/01, 39(1), pp. 56–63. doi: 10.1159/000381914.

- Goldstein, J. A. et al. (2020) "Maternal-Fetal Inflammation in the Placenta and the Developmental Origins of Health and Disease," *Front Immunol.* 2020/12/08, 11, p. 531543. doi: 10.3389/fimmu.2020.531543.
- Hermodson, M. (1996) "Current protocols in protein science, edited by J.E. Coligan, B.M. Dunn, H.L. Ploegh, D.W. Speicher, and P.T. Wingfield. New York: Wiley, 1995, 864 pages (core) + 576 pages (4 supplements)/year (updated looseleaf), print and CD-ROM," *Proteins: Structure, Function, and Bioinformatics*, 24(3), p. 409. doi: <https://doi.org/10.1002/prot.340240303>.
- Hung, C. W. et al. (2007) "Collision-induced reporter fragmentations for identification of covalently modified peptides," *Anal Bioanal Chem.* 2007/08/11, 389(4), pp. 1003–1016. doi: 10.1007/s00216-007-1449-y.
- Huppertz, B. et al. (2008) "Longitudinal determination of serum placental protein 13 during development of preeclampsia," *Fetal Diagn Ther.* 2008/08/30, 24(3), pp. 230–236. doi: 10.1159/000151344.
- Jirak, P. et al. (2019) "Clinical implications of fetuin-A," *Adv Clin Chem.* 2019/02/25, 89, pp. 79–130. doi: 10.1016/bs.acc.2018.12.003.
- Johannes, L., Jacob, R. and Leffler, H. (2018) "Galectins at a glance," *J Cell Sci.* 2018/05/03, 131(9). doi: 10.1242/jcs.208884.
- Kelly, S. M., Jess, T. J. and Price, N. C. (2005) "How to study proteins by circular dichroism," *Biochim Biophys Acta.* 2005/07/20, 1751(2), pp. 119–139. doi: 10.1016/j.bbapap.2005.06.005.
- Kliman, H. J. et al. (2012) "Placental protein 13 and decidual zones of necrosis: an immunologic diversion that may be linked to preeclampsia," *Reprod Sci.* 2011/10/13, 19(1), pp. 16–30. doi: 10.1177/19337191111424445.
- Laaf, D. et al. (2019) "Galectin-Carbohydrate Interactions in Biomedicine and Biotechnology," *Trends Biotechnol.* 2018/11/11, 37(4), pp. 402–415. doi: 10.1016/j.tibtech.2018.10.001.
- Di Lella, S. et al. (2010) "Linking the structure and thermal stability of beta-galactoside-binding protein galectin-1 to ligand binding and dimerization equilibria," *Biochemistry.* 2010/07/30, 49(35), pp. 7652–7658. doi: 10.1021/bi100356g.

- Leonidas, D. D. et al. (1998) "Structural basis for the recognition of carbohydrates by human galectin-7," *Biochemistry*. 1998/10/07, 37(40), pp. 13930–13940. doi: 10.1021/bi981056x.
- Li, C. H. et al. (2011) "Applications of circular dichroism (CD) for structural analysis of proteins: qualification of near- and far-UV CD for protein higher order structural analysis.," *Journal of pharmaceutical sciences*, 100(11), pp. 4642–4654. doi: 10.1002/jps.22695.
- Loser, K. et al. (2009) "Galectin-2 suppresses contact allergy by inducing apoptosis in activated CD8+ T cells.," *Journal of immunology (Baltimore, Md. : 1950)*, 182(9), pp. 5419–5429. doi: 10.4049/jimmunol.0802308.
- Marini, M. et al. (2011) "Distribution of sugar residues in human placentas from pregnancies complicated by hypertensive disorders," *Acta Histochemica*, 113(8), pp. 815–825. doi: 10.1016/j.acthis.2010.12.001.
- McMaster, M. T. and Fisher, S. J. (2003) "Placental Development," in Henry, H. L. and Norman, A. W. B. T.-E. of H. (eds.). New York: Academic Press, pp. 213–219. doi: <https://doi.org/10.1016/B0-12-341103-3/00247-3>.
- Meggyes, M. et al. (2014) "Peripheral blood TIM-3 positive NK and CD8+ T cells throughout pregnancy: TIM-3/galectin-9 interaction and its possible role during pregnancy.," *PloS one*, 9(3), p. e92371. doi: 10.1371/journal.pone.0092371.
- Menkhorst, E. M. et al. (2014) "Galectin-7 acts as an adhesion molecule during implantation and increased expression is associated with miscarriage.," *Placenta*, 35(3), pp. 195–201. doi: 10.1016/j.placenta.2014.01.004.
- Miller, M. C. et al. (2020) "Structural insight into the binding of human galectins to corneal keratan sulfate, its desulfated form and related saccharides," *Sci Rep*. 2020/09/26, 10(1), p. 15708. doi: 10.1038/s41598-020-72645-9.
- Mor, G., Aldo, P. and Alvero, A. B. (2017) "The unique immunological and microbial aspects of pregnancy," *Nat Rev Immunol*. 2017/06/20, 17(8), pp. 469–482. doi: 10.1038/nri.2017.64.
- Nakahara, S., Oka, N. and Raz, A. (2005) "On the role of galectin-3 in cancer apoptosis,"

- Apoptosis. 2005/04/22, 10(2), pp. 267–275. doi: 10.1007/s10495-005-0801-y.
- Nesvizhskii, A. I. et al. (2003) “A Statistical Model for Identifying Proteins by Tandem Mass Spectrometry,” *Analytical Chemistry*, 75(17), pp. 4646–4658. doi: 10.1021/ac0341261.
- Niger, C., Malassine, A. and Cronier, L. (2004) “Calcium channels activated by endothelin-1 in human trophoblast,” *J Physiol*. 2004/09/11, 561(Pt 2), pp. 449–458. doi: 10.1113/jphysiol.2004.073023.
- Pettersen, E. F. et al. (2004) “UCSF Chimera--a visualization system for exploratory research and analysis,” *J Comput Chem*. 2004/07/21, 25(13), pp. 1605–1612. doi: 10.1002/jcc.20084.
- Rabinovich, G. A. et al. (2002) “Galectins and their ligands: Amplifiers, silencers or tuners of the inflammatory response?,” *Trends in Immunology*, 23(6), pp. 313–320. doi: 10.1016/S1471-4906(02)02232-9.
- Rustiguel, J. K. et al. (2016) “Full-length model of the human galectin-4 and insights into dynamics of inter-domain communication,” *Sci Rep*. 2016/09/20, 6, p. 33633. doi: 10.1038/srep33633.
- Sakakura, M. et al. (2018) “Structural mechanisms for the S-nitrosylation-derived protection of mouse galectin-2 from oxidation-induced inactivation revealed by NMR,” *FEBS J*. 2018/02/03, 285(6), pp. 1129–1145. doi: 10.1111/febs.14397.
- Sammar, M. et al. (2019) “Galectin 13 (PP13) Facilitates Remodeling and Structural Stabilization of Maternal Vessels during Pregnancy,” *Int J Mol Sci*. 2019/07/03, 20(13). doi: 10.3390/ijms20133192.
- Saraboji, K. et al. (2012) “The carbohydrate-binding site in galectin-3 is preorganized to recognize a sugarlike framework of oxygens: ultra-high-resolution structures and water dynamics,” *Biochemistry*. 2011/11/25, 51(1), pp. 296–306. doi: 10.1021/bi201459p.
- Sgambati, E. et al. (2007) “Distribution of the glycoconjugate oligosaccharides in the human placenta from pregnancies complicated by altered glycemia: lectin histochemistry,” *Histochem Cell Biol*. 2007/07/27, 128(3), pp. 263–273. doi: 10.1007/s00418-007-0312-8.

- Si, Y., Yao, Y., et al. (2021) "Human galectin-16 has a pseudo ligand binding site and plays a role in regulating c-Rel-mediated lymphocyte activity," *Biochim Biophys Acta Gen Subj.* 2020/10/05, 1865(1), p. 129755. doi: 10.1016/j.bbagen.2020.129755.
- Si, Y., Li, Y., et al. (2021) "Structure-function studies of galectin-14, an important effector molecule in embryology," *FEBS J.* 2020/06/12, 288(3), pp. 1041–1055. doi: 10.1111/febs.15441.
- Sindrewicz, P. et al. (2019) "Intrinsic tryptophan fluorescence spectroscopy reliably determines galectin-ligand interactions," *Sci Rep.* 2019/08/16, 9(1), p. 11851. doi: 10.1038/s41598-019-47658-8.
- St-Pierre, Y., Doucet, N. and Chatenet, D. (2018) "A New Approach to Inhibit Prototypic Galectins," *Trends in Glycoscience and Glycotechnology*, 30(172), pp. SE155–SE165. doi: 10.4052/tigg.1730.1se.
- Su, J., Wang, Y., et al. (2018) "Galectin-13, a different prototype galectin, does not bind beta-galacto-sides and forms dimers via intermolecular disulfide bridges between Cys-136 and Cys-138," *Sci Rep.* 2018/01/19, 8(1), p. 980. doi: 10.1038/s41598-018-19465-0.
- Su, J., Cui, L., et al. (2018) "Resetting the ligand binding site of placental protein 13/galectin-13 recovers its ability to bind lactose," *Biosci Rep.* 2018/11/11, 38(6). doi: 10.1042/BSR20181787.
- Than, N. G. et al. (2004) "Functional analyses of placental protein 13/galectin-13," *Eur J Biochem.* 2004/03/11, 271(6), pp. 1065–1078. doi: 10.1111/j.1432-1033.2004.04004.x.
- Than, N. G. et al. (2009) "A primate subfamily of galectins expressed at the maternal-fetal interface that promote immune cell death," *Proc Natl Acad Sci U S A.* 2009/06/06, 106(24), pp. 9731–9736. doi: 10.1073/pnas.0903568106.
- Than, N. G. et al. (2014) "Placental Protein 13 (PP13) - A Placental Immunoregulatory Galectin Protecting Pregnancy," *Front Immunol.* 2014/09/06, 5, p. 348. doi: 10.3389/fimmu.2014.00348.
- Trowsdale, J. and Betz, A. G. (2006) "Mother's little helpers: mechanisms of maternal-fetal tolerance," *Nat Immunol.* 2006/02/17, 7(3), pp. 241–246. doi: 10.1038/ni1317.

- Unverdorben, L. et al. (2015) "Galectin-13/PP-13 expression in term placentas of gestational diabetes mellitus pregnancies," *Placenta*. 2014/12/17, 36(2), pp. 191–198. doi: 10.1016/j.placenta.2014.11.019.
- Vasta, G. R. et al. (2012) "Galectins as self/non-self recognition receptors in innate and adaptive immunity: an unresolved paradox," *Front Immunol*. 2012/07/20, 3, p. 199. doi: 10.3389/fimmu.2012.00199.
- Villeneuve, C. et al. (2011) "Mitochondrial proteomic approach reveals galectin-7 as a novel BCL-2 binding protein in human cells," *Mol Biol Cell*. 2011/02/04, 22(7), pp. 999–1013. doi: 10.1091/mbc.E10-06-0534.
- Vokalova, L. et al. (2020) "Placental Protein 13 (Galectin-13) Polarizes Neutrophils Toward an Immune Regulatory Phenotype," *Front Immunol*. 2020/03/03, 11, p. 145. doi: 10.3389/fimmu.2020.00145.
- Wdowiak, K. et al. (2018) "Galectin Targeted Therapy in Oncology: Current Knowledge and Perspectives," *Int J Mol Sci*. 2018/01/11, 19(1). doi: 10.3390/ijms19010210.
- Yang, T. et al. (2020) "Galectin-13/placental protein 13: redox-active disulfides as switches for regulating structure, function and cellular distribution," *Glycobiology*. 2019/10/05, 30(2), pp. 120–129. doi: 10.1093/glycob/cwz081.
- You, J.-L. et al. (2018) "A potential role of galectin-1 in promoting mouse trophoblast stem cell differentiation.," *Molecular and cellular endocrinology*, 470, pp. 228–239. doi: 10.1016/j.mce.2017.11.003.